CHARACTERIZATION OF THE EVOLUTION OF A RELOCATED TIDAL INLET: MASON INLET, NORTH CAROLINA

John M. Welsh

A Thesis Submitted to the
University of North Carolina at Wilmington in Partial Fulfillment
Of the Requirements for the Degree of
Master of Science

Department of Earth Sciences

University of North Carolina at Wilmington

2004

Approved by

Advisory Committee

Paul A. Thayer   Lynn A. Leonard

William J. Cleary
Chair

Accepted by

Robert D. Roer
Dean, Graduate School

This thesis has been prepared in a style and format

consistent with

The Journal of Coastal Research

TABLE OF CONTENTS

ABSTRACT

Between January and April 2002, Mason Inlet, situated between Figure Eight Island and Wrightsville Beach, N.C. was artificially relocated 2,800 ft updrift of its most recent position at the southern terminus of a migrating barrier spit. Relocation was chosen from several coastal management options due to increased backbarrier infilling and southerly migration of the inlet that imminently threatened a resort complex and infrastructure on northern Wrightsville Beach. The relocated Mason Inlet provides an ideal site to study the evolution and impacts of a recently relocated system from its inception while simultaneously assessing the relative success of the project. Techniques such as ADCP, RTK GPS, and GIS-based analyses served as tools in the collection of data pertaining to a variety of inlet parameters.

Cumulative erosion measured along neighboring shoreline reaches was induced by inlet relocation and subsequent formation of the ebb-tidal delta coupled with channel migration. Key indicators suggest that the system remains flood dominant. Noticeable infilling of the backbarrier persists along with ebb durations exceeding flood durations and flood flow volumes exceeding ebb volumes. JARRETT's (1976) theoretical equation relating tidal prism (T_P) and cross-sectional area (A_C) appears to be a useful tool for estimation of the relocated Mason Inlet's T_P. However, ebb-tidal delta volume after 1.6 years remains well below the equilibrium volume predicted by WALTON and ADAMS' (1976) model. Future modification (e.g. dredging feeder channels) to the system will be needed in order to mitigate the infilling nature of the inlet that historically has led to increased migration to the southwest. Failure to contain the inlet within the proposed “inlet corridor” will result in an unsuccessful relocation effort.

ACKNOWLEDGEMENTS

This thesis would not have been possible without the aid of countless individuals. Foremost, I would like to express my utmost appreciation to my entire family, especially my parents, James and Suzanne Welsh, for their instilled confidence and incessant support of my educational endeavors. A genuine debt of gratitude is extended to Dr. W. Cleary for imparting his knowledge and expertise and providing me with an exemplary graduate-level experience. The knowledge bestowed under his advisement has proven to be an invaluable tool in completing this project and preparing for future career opportunities. Appreciation is expressed to Dr. L. Leonard and Dr. P. Thayer, committee members, for their encouragement, advice, and diligence in seeing to completion the success of this project. I would like to thank the members of the Coastal Geology Laboratory, specifically, Ben McGinnis, Chester Jackson, Adam Knierim, Kenny Willson, David Doughty, and Leighann Budde, for their friendship foremost, loyalty, advice, and willingness to aid a colleague. Thanks to one of my best friends, Dan Orr, for your moral support and encouragement over these last three years.

Spencer Rogers, of N.C. Sea Grant, provided countless contacts, information, and advice related to this investigation and was considered an invaluable resource. Special thanks are also extended to Chris Gibson of Gahagan & Bryant Associates for graciously providing detailed bathymetric data and aerial photographs, Lyn Jack of the U.S. Army Corps of Engineers, Wilmington District, for the unlimited access to aerial photographs, and Karyn Erickson of Erickson Consulting Engineers, for providing water-level data. I would also like to thank the UNCW Department of Earth Sciences for providing financial support during my graduate tenure and the UNCW Center for Marine Science for making boats and equipment readily available during the field component of my research. The U.S. Army Corps of Engineers Coastal Inlets

Research Program and N.C. Sea Grant provided funding for a portion of the research invested in this study.

LIST OF TABLES

LIST OF FIGURES

INTRODUCTION

Tidal inlets are corridors between adjacent barrier islands that act as pathways for exchanging water, sediment, and nutrients between the open ocean and estuaries. Each inlet is part of a sand-sharing system, and plays a major role in the coastal sand budget by retaining large volumes of sediment from the littoral system (BRUUN and GERRITSEN, 1959; FITZGERALD, 1982; OERTEL, 1975). Tidal prism and the local wave climate of an inlet system control the extent to which these systems interrupt the littoral drift and store sand (HAYES, 1980).

Inlets are dynamic systems and are constantly in a state of flux and as a result pose a heightened threat to adjacent coastal communities. Twenty tidal inlets punctuate the extensive shoreline (320 miles) of North Carolina and currently comprise approximately one percent of North Carolina's shoreline (CLEARY, 1996). In Onslow Bay, situated between Cape Lookout and Cape Fear and containing approximately one-third of the 320-mile extent of North Carolina's shoreline, inlets have influenced sixty-five percent of the barrier island shorelines during the past two hundred years (CLEARY, 1996). The great majority of the critical erosion zones identified along the shoreline are associated with inlet systems. The negative impacts within these inlet-influenced critical erosion zones are exacerbated when the tidal inlet is a migrating system.

Most of North Carolina's inlets have been modified to some extent as a result of improved navigation via channel maintenance and removal of sand for beach nourishment. Hard stabilization techniques (engineering solution) by way of jetties or groins are traditionally used in the United States; however, North Carolina implemented a general statute, in 1984, that prohibits the use of hardened erosion-control structures along its coastline. As a result, soft protection techniques (e.g. dredging, beach nourishment, and sandbag installations) have become the mainstays of North Carolina's engineering solutions to these coastal hazard scenarios. Reasons for practices such as these are typically associated with the mitigation of shoreline erosion. Large-scale modification of inlets, associated with relocation or jetty emplacement, commonly alters the parameters (e.g. cross-sectional area, tidal prism, etc.) of an inlet and can result in substantial erosion of neighboring shorelines (CLEARY *et al*., 1989; CLEARY and MARDEN, 1999). Concern over management issues (e.g. artificial inlet relocation) related to these modifications has increased due to the severe impacts associated with these alterations and the future modifications (e.g. dredging) slated for most of North Carolina's inlets.

Knowledge of how large-scale modification alters the physical parameters, current dominance, basin filling characteristics, as well as the impact on the offshore portion of specific inlet systems in southeastern North Carolina is lacking. A key element in evaluating the performance of an inlet is applying the linear regression relationships derived by JARRETT (1976) and WALTON and ADAMS (1976) for equilibrated inlet systems to the new system. This thesis provides a framework from which the ramifications of inlet relocation on the neighboring oceanfront shoreline, tidal prism, inlet-related sand shoal budget, and current dominance will be better understood. The relocated Mason Inlet provides an ideal site to study the evolution and impacts of a recently relocated system from its inception by comparing the actual measured and derived values to predicted values obtained from regression equations associated with key inlet parameters.

Objectives

The specific objectives of this study are to:

- Analyze four sets of pre-relocation and seven sets of post-relocation aerial photographs within a geographic information system (GIS) to identify morphologic changes associated with the inlet's neighboring shoreline morphology and the extent of sand shoals comprising the new and abandoned flood and ebb deltas.
- Monitor the changes in volume and area of the new ebb-tidal delta, and characterize changes in cross-sectional area, tidal prism, aspect ratio (width:depth), and other parameters of the inlet over a 1.6-year period following the relocation.
- Utilize the theoretical equations of WALTON and ADAMS (1976) and JARRETT (1976) to predict specific physical inlet parameters such as throat cross-sectional area, tidal prism, and ebb-tidal delta volume. Compare the predicted values to those corresponding values that were calculated from directly measured field data. Ultimately determine the applicability of these theoretical models to this particular inlet system following a relocation effort.
- Quantify volume changes and track the migration of a flood shoal within Banks Channel over a six-week period to monitor tidal and wave influence on sediment transport within a secondary feeder channel connecting the inlet to the Atlantic Intracoastal Waterway (AIWW).
- Monitor currents within the inlet throat, Banks Channel, and Mason Creek using an Acoustic Doppler Current Profiler (ADCP) to ascertain what distribution of flow passes through feeder channels of Banks Channel and Mason Creek, the primary navigational corridor connecting the inlet to the AIWW.

Site Description

Mason Inlet, situated in Onslow Bay along North Carolina's southeast coast, lies between Figure Eight Island to the northeast and Wrightsville Beach to the southwest (Figure 1). This region is characterized by HAYES (1994) as microtidal and wave-dominated with mixed semi-diurnal tides. The backbarrier region between the AIWW and Mason Inlet is the Middle Sound Estuary, which consists mostly of marsh incised by tidal creeks. Mason Creek and Banks Channel, two primary tidal channels within the estuary, provide the only navigable connection between the inlet and the AIWW.

Mean wave height and period in this region are 2.6 ft and 7.9 seconds, respectively (JARRETT, 1977). The measured tidal range of this system has a mean range of 3.28 ft, which increases to 3.93 ft under spring tide conditions and decreases to 2.66 ft under neap tide conditions. KNIERIM (2003) noted that the mean range for Rich Inlet to the northeast measured 3.54 ft. Mean sea level was determined to exist at an elevation of -0.31 ft (North American Vertical Datum 1988 (NAVD 88)). The dominant direction of wave propagation is from the east-northeast and comprises 64% of the total wave energy that affects this area. These waves result from the extra-tropical storms that occur during the fall and winter (FINLEY, 1976). Net longshore sediment transport is in the southerly direction and occurs at a rate of approximately 769,000 yd^3/yr (USACE, 1982).

Background

A geomorphic and historic account of inlet activity associated with Mason Inlet (Figure 1) and the surrounding area determined that several migrating inlets had cycled through the region during the past 200 years as evidenced by a series of narrow, elongated marsh islands

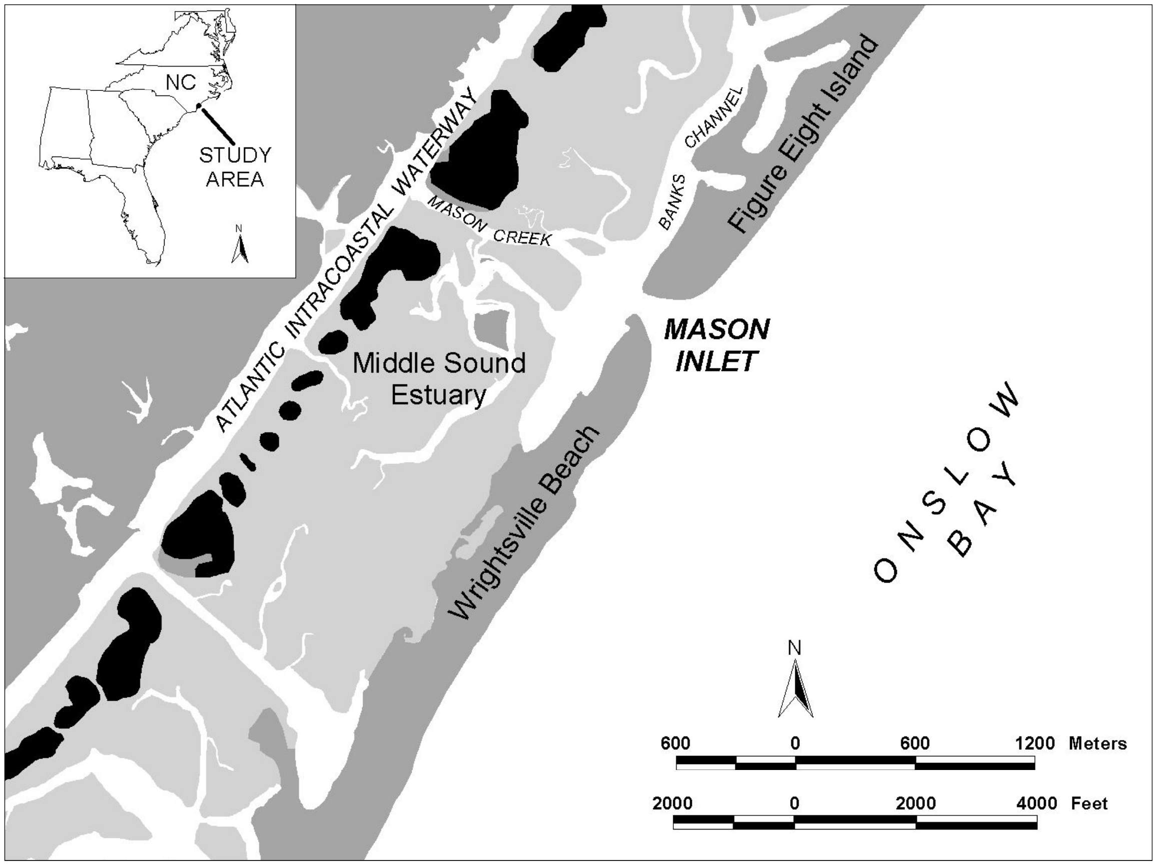

Figure 1. Location map of the study area. Dark features are dredge spoil islands.

situated within the backbarrier lagoon (CLEARY and MARDEN, 1999). Barren Inlet, a predecessor to Mason Inlet, known also as Wrightsville or Moores Inlet, opened in 1733 along the southern portion of Figure Eight Island and migrated to the southwest prior to the opening of Mason Inlet in 1888 (CLEARY *et al*., 1979; BROOKS, 1988; CLEARY and MARDEN, 1999; JOHNSEN *et al*., 1999; FREEMAN, 2001; JACKSON, 2004). Between 1888 and 1965, Mason Inlet was situated between Figure Eight Island and Shell Island whereas Barren Inlet to the south was positioned between Shell Island and Wrightsville Beach (JACKSON, 2004). The artificial closure of Barren Inlet in 1965 by the U.S. Army Corps of Engineers (USACE) resulted in the merger of Shell Island with Wrightsville Beach into one contiguous island. Mason Inlet continued to migrate to the southwest and separated Figure Eight Island from an extended Wrightsville Beach.

Since the early 1900's, the inlet has exhibited a net migration pattern to the southwest stretching along a one-mile corridor. Although the predominant nature of inlet migration has been in the southwesterly direction, short-term reversals have occurred. Historically, spanning decadal time periods (1940's to 1990's), inlet migration rates have varied greatly and are thought to be controlled by the characteristic shoaling nature of the inlet and reduction in tidal prism as migration perpetuates (CLEARY and FITZGERALD, 2003). Migration rates between the mid-1960's and 1990's ranged from 0 to 295 ft/yr. The highest rates during this time period occurred during the mid-1990's when the inlet system experienced a marked influx of sediment that resulted in shoaling of the inlet's interior channels along with a subsequent reduction in cross-sectional area and tidal prism. Reduction of the inlet's tidal exchange capacity allowed alongshore drift to assume the dominant role in determining the inlet's location. Between 1974 and 1996, the inlet channel migrated southwest approximately 3,609 ft, at an average rate of 164 ft/yr (CLEARY and MARDEN, 1999). Migration of the opposing inlet shoulders occurred at varying rates with the updrift margin moving 20 ft/yr faster than the downdrift margin during this particular period. Drastic changes in the planform of the adjacent barrier islands resulted from migration of the inlet (BROOKS, 1988).

By 1997, the inlet channel had migrated to a position within 65 ft of a $22 million resort complex (Shell Island Resort) located on the northern terminus of Wrightsville Beach (Figure 2a). The position of the inlet at that time not only imminently threatened the resort but also posed a potential future problem for approximately 650 properties, including single-family homes and several condominium complexes located further to the southwest of the resort. The Shell Island Homeowners Association obtained a variance from the N.C. Coastal Resources Commission (NCCRC) and N.C. Division of Coastal Management (NCDCM) on February 4, 1997 to build a large geotextile revetment (combination of sandbags and geo-tubes) along Mason Inlet's southern channel bank to protect the imminently threatened resort building (Figure 2a).

Stabilization of the inlet's southern margin caused the inlet throat to adjust accordingly. The throat cross-sectional area in 1996, prior to sandbag and geo-tube emplacement, measured 2,207 ft^2 and decreased by 36% over the next two years. The inlet channel's depth scoured from 6.6 to 11.2 ft over the same period. By 2001, an additional 46% reduction (1,410 ft^2 to 764 ft^2) in cross-sectional area occurred as continued elongation of the updrift spit led to encroachment of the spit upon the ebb channel and the southern margin that remained in place (CLEARY and FITZGERALD, 2003).

In order to understand changes to the inlet over the past thirty years, knowledge of how the tidal prism fluctuated must be addressed. CLEARY and FITZGERALD (2003) noted a reduction in size of the inlet since the late-1970's. Based on O'BRIEN's (1931, 1969) empirical model that relates inlet throat cross-sectional area to tidal prism, the noted reduction in size of the inlet was attributed to a diminished tidal prism (CLEARY and FITZGERALD, 2003). Over this time period, Mason Inlet experienced a shoaling trend within the feeder channels and flood shoal complexes positioned within the backbarrier portion of the system. Mason Creek experienced a high degree of sedimentation during the late-1980's through the mid-1990's. FREEMAN (2001) recorded shorter flood durations (6.06 hrs) than ebb (6.36 hrs) with faster flood (2.85 ft/s) than ebb (2.20 ft/s) current velocities from within the creek in 1998. Measurements such as these indicate flood dominance and support the observation of net sediment transport to the backbarrier portion of the system. Increased shoaling of the lagoon behind the barrier islands eventually diminishes the area that the backbarrier bay encompasses. As the bay area is diminished a notable reduction in the inlet's tidal prism is expected (FITZGERALD, 1996). Previous studies of Mason Inlet support this assumption. A sand accumulation rate of 75,861 yd^3/yr was estimated to have occurred from 1996 to 1999 within the interior feeder channels (ATM, 2000). A noticeable 63% reduction (67.1×10^6 ft^3 to 24.7×10^6 ft^3) in tidal prism occurred between 1995 and 1999 (CLEARY, 2003; ATM, 2000).

Initially, the installation of sandbags along the southern margin of the inlet was perceived as a short-term solution to protect the infrastructure of Shell Island against the inlet's migration. However, as a condition of the variance, a long-term solution was needed to deal with this issue. The deadline for removal of the sandbags was initially set for September of 1999.

The Mason Inlet Preservation Group (MIPG) formed in 1998. In conjunction with New Hanover County several "long-term" options were explored. The proposed solutions included a "no-action" proposal that would allow the inlet to migrate uninhibited at the expense of the infrastructure located downdrift of the inlet. Another proposal called for "inlet-closure". The environmental ramifications of this scenario, which would result in reduced flushing between the Atlantic Intracoastal Waterway (AIWW) and the ocean by combining Figure Eight Island with Wrightsville Beach, culminated in its rejection by the county. The third proposal of "inlet-relocation" sought to reposition the inlet updrift of its current location. Ultimately, Applied Technology and Management, Inc. (ATM) was contracted by the county in 1998 to devise a workable inlet relocation project.

An extension of the variance was issued that allowed the sandbags and geo-tubes to remain in-place until September 2000 to provide more time to devise a feasible solution. The issue gained national attention after the extension expired, and the homeowners of the resort complex refused to remove the sandbags. Consequently, several variance extensions were granted, and a final deadline to remove the sandbags and geo-tubes was set for December 2001.

ATM engineers designed a plan to reposition Mason Inlet 2,800 feet north of its current location and included excavation of a new inlet channel, realignment of Mason Creek, and closure of the former Mason Inlet. A large-scale hydrodynamic model showing the potential project impacts on wildlife, fisheries and other biological resources, was completed. It was not until November 2001 that the USACE, Wilmington District issued a provisional permit to New Hanover County for the proposed relocation of Mason Inlet. The National Fish and Wildlife Coordination Act and the Clean Water Act required that the USACE include certain conditions on the permit to protect fish and wildlife resources. Finally, on January 10, 2002 the USACE, New Hanover County, and local environmental agencies agreed on a contract that met all the interests that were necessary for the relocation effort.

The 2D hydrodynamic model, used by ATM, allowed engineers to simulate and design the ideal configuration of the new inlet channel. For the purposes of the project, the relocation design recommended the inlet channel should be cut approximately 2,800 feet northeast or updrift of its December 2001 (pre-project) location and have a cross-sectional area of 5,000 ft^2. The major goals established for the project design included: (1) protecting the infrastructure and resort complex on Wrightsville Beach and nourishing the updrift shoreline of Figure Eight Island, (2) reducing the impacts to the surrounding marsh and native bird and marine life habitats, (3) mitigating any hydrodynamic effects on the neighboring Rich Inlet to the northeast and Masonboro Inlet to the southwest, and (4) creating, within reason, a relatively natural stable inlet to be contained within a 1,000-foot "inlet corridor" (ERICKSON *et al*., 2003).

The construction phase for the relocation began in January of 2002 and extended until April 15, 2002. The new inlet channel was excavated across the southern spit of Figure Eight Island directly in-line with the position of Mason Creek (Figure 2e) in order to maximize flushing between the ocean and the AIWW. Excavation to construct this design template required the removal of 340,000 yd^3 of sand from the new inlet channel and 145,000 yd^3 from Mason Creek (ERICKSON *et al*., 2003). An additional 335,000 yd^3 was removed from an area located directly landward of the new inlet channel to provide a catchment basin for the newly developing flood shoal and to prevent excess amounts of sediment from being transported into the AIWW. Approximately 400,000 yd^3 of the excavated sand was used to nourishment 2.5 miles of shoreline along the southern end of Figure Eight Island (Figure 2c).

Officially, the relocated Mason Inlet channel was opened during a neap tidal phase prior to the beginning of an ebb tidal flow on the afternoon of March 7, 2002 (Figure 2d). The closure of the original inlet channel to the southwest was completed a week later on March 14, 2002. An estimated 270,000 yd^3 of material was used to plug the original inlet (ERICKSON *et al*., 2003).

Figure 2. Photographs illustrating (a) Shell Island Resort, (b) construction phase, (c) beach nourishment of Figure Eight Island, (d) inlet opening, (e and f) old inlet closure, (g) original inlet closed and ebb shoal collapse, associated with the relocation of Mason Inlet. Photographs courtesy of ATM and Dr. W. Cleary.

The original ebb-tidal delta was allowed to naturally collapse against this section of shoreline under wave action and nourish the beach fronting the resort complex (Figure 2g). A monitoring program to track inlet evolution was developed in accordance with the New Hanover County Mason Inlet Management Plan and Environmental Assessment, the USACE Permit #19901052, and the N.C. Department of Environmental Resources Permit #151-01 (GBA, 2002). ATM conducted two partial physical monitoring surveys, one prior to and one during the construction phase of the relocation effort. Gahagan andBryant Associates, Inc. (Wilmington, N.C. Office), contracted by the county to execute quarterly physical monitoring surveys of the inlet system during the first year following relocation and bi-annually thereafter, began monitoring efforts in July 2002. The goal of this monitoring effort was to address the relocation's impact on the neighboring oceanfront shoreline and the shoaling characteristics within the inlet system. Supplemental to these efforts, the USACE Coastal Inlets Research Program (CIRP) funded data collection in association with Erickson Consulting Engineers, Inc. (ECE) to monitor the circulation patterns in the backbarrier feeder channels and development of the ebb-tidal delta. USACE instruments deployed by ECE, at the time of writing this thesis, are no longer collecting data within the inlet system.

Previous Works

Inlet relocation, as a viable management option, is a relatively recently-employed technique that has been made available to coastal managers under site-specific conditions. Completed relocation efforts have exclusively dealt with migrating inlets that have posed some degree of threat to the surrounding coastal zone (usually near infrastructure) that borders an inlet. Relocation may be classified as a soft-solution management option. Rather than attempting to force the system to behave in a manner unsuitable for the area, the operation works in tandem with the natural processes by artificially recreating the evolution of a migrating inlet. As a result, the environmental impacts on the surrounding system are diminished greatly by comparison to other hard stabilization techniques (e.g. jetty emplacement). Only a few examples of inlet relocation exist worldwide. The first relocation found in the literature was conducted on St. Augustine Inlet situated along the northeastern coast of Florida. This inlet was artificially relocated approximately 1,200 ft north of its original position in 1940. MARINO and MEHTA (1987) describe the morphologic changes of the ebb shoals and oceanfront shoreline associated with this project and the installation of a dual jetty structure between 1941 and 1957. Ironically, Mason Inlet is not the first small, microtidal inlet in North Carolina to be relocated. Tubbs Inlet was relocated in January of 1970. Unfortunately, no studies exist that deal with the morphologic and hydrodynamic evolution of the inlet. However, CLEARY and MARDEN (1999) determined that after a period of adjustment the inlet began to migrate opposite its historic migration direction and the regional net littoral drift direction. This new migration trend continues to date. Although the reasons for it are not completely understood, reversal in migration direction is likely due to alterations in the interior feeder channel dominance (BUDDE and CLEARY, 2004). Stump Pass, a relatively small inlet situated between Manasota Key and Knight Island, Florida, was relocated 3,200 ft north in 2003 (MICHAEL POFF, *pers. comm*.).

Published studies dealing with monitoring the effects of relocated tidal inlets along U.S. and foreign coastlines are rare. Studies of the 1983 relocation of Captain Sam's Inlet (mesotidal setting) near Charleston, South Carolina, include KANA and MASON's (1988) study that monitored the evolution and growth of the ebb-tidal delta, and the KANA *et al*. (1987) study that determined a sediment budget for this system. However, as the inlet evolved it managed to migrate back to its approximate 1982 position twelve years after the relocation (KANA and MCKEE, 2003). Consequently, another artificial relocation of the inlet occurred in 1996. Both inlet relocation efforts are summarized in KANA and MCKEE (2003).

The study of Ancão Inlet's 1997 relocation, along the mesotidal, Ria Formosa barrier island system, in Portugal by VILA *et al*. (1999) determined that dramatic volumetric changes occurred during the first year of evolution, with the enlargement of the inlet and the formation of well-developed flood and ebb deltas. A more comprehensive study of the Ria Formosa system was undertaken by CONCEJO (2003) that expanded upon the relocation impacts on Ancão Inlet and included observations pertaining to the 1999 artificial relocation of Fuzeta Inlet. As a result of this study CONCEJO (2003) formulated assesment criteria for determining the success of an inlet relocation effort within the Ria Formosa system. According to the study and based on the assessment scale, the relocation of Ancão Inlet was considered a success. However, the Fuzeta Inlet relocation failed to meet the requirements necessary for a successful relocation effort because the area was soon plagued with the same problems it faced prior to the effort with the inlet swiftly migrating eastwardly. CONCEJO (2003) determined that the most important factor for a relocation action to suceed was the correct choice of where to reopen the inlet.

Studies such as these are extremely important because they serve as case-studies for future inlet modifications. The methods employed and the relative success of previous relocation efforts may be used to identify site-specific locations where inlet relocation may be viable. Also, the importance of relocation studies pertaining to an assortment of tidal settings (e.g. microtidal) will be beneficial to these efforts. Already, future inlet relocations are under consideration. For example, the details of a possible relocation of Fire Island Inlet along Long Island, New York, is provided by KRAUS *et al.* (2003). Although not a relocation, a feasibility study has been completed on the potential reopening of Midnight Pass, a historically migrating inlet, along the Gulf coast of Sarasota County, Florida (DAVIS, *et al*., 1987; Erickson Consulting Engineers (ECE), 2003).

In order for an inlet relocation to be successful, an initial comprehensive study of the inlet's history must be accomplished incorporating as much of the historical data as possible. Additionally, certain fundamental parameters of an inlet system must be monitored as the new inlet system evolves to understand how relocation affects hydrodynamic and morphologic changes.

Regression analyses of related morphologic and hydraulic characteristics of tidal inlets have been relatively successful in modeling of inlet systems. These relationships between inlet parameters and processes have aided in the research of inlets worldwide (KANA *et al*., 1999). JARRETT (1976) refined LECONTE's (1905) and O'BRIEN's (1931 and 1969) relationship between tidal prism and inlet cross-sectional area. WALTON and ADAMS (1976) derived an empirical relationship between ebb delta volume and tidal prism.

Only recently has the relocation of an inlet become a viable solution for coastal managers. Worldwide, limited studies exist that pertain to the impacts of inlet relocations. The study of Mason Inlet's relocation provides a unique opportunity to further the understanding of the impacts that these efforts can impose on not only the neighboring shoreline segments but on the hydrodynamics and sediment budget affected by this process. Techniques utilizing ADCP, Real-time kinematic (RTK) global positioning system (GPS), and geographic information system (GIS) technologies were used in this study.

The approach of this study is based on interpreting and drawing meaningful conclusions from field data and derived values to track the performance of the system. Determining potential relationships between specific inlet parameters and the applicability of those relationships to established regression analyses is a main tenet of the study. This study of Mason Inlet's relocation is unique when compared to other studies that have collected data strictly from a monitoring and engineering objective. The study's analytical approach seeks to understand the individual processes impacting the system and relating them in order to understand the system as a whole.

METHODOLOGY

The investigation incorporated the detailed collection of photogrammetric, topo-bathymetric, hydrographic, and tidal data. All tidal and topo-bathymetric data were referenced horizontally (North Carolina State Plane 1983) and vertically to NAVD 88. A Remote Data Systems' Ecotone-80 model water-level meter was deployed within Banks Channel approximately 2,400 ft from the inlet throat in order to determine the range and duration of tides (Figure 3). Water-level measurements were collected at ten-minute intervals within an internal data logger. The Microsoft® Excel™ software package was utilized in post-processing all tidal data for management and analysis. Identification of parameters such as Mean Sea Level (MSL); Spring, Neap, and mean tidal ranges; and flood/ebb flow durations, involved the filtration of data to determine successive high and low water levels.

ADCP and Flow Dynamics

A vessel-mounted RD Instruments® (RDI) Workhorse Monitor™ 1200 kHz ADCP was used in the collection of all flow data within the inlet throat, Banks Channel, and Mason Creek (Figure 3). This data collection process differs uniquely from the methodology employed by the

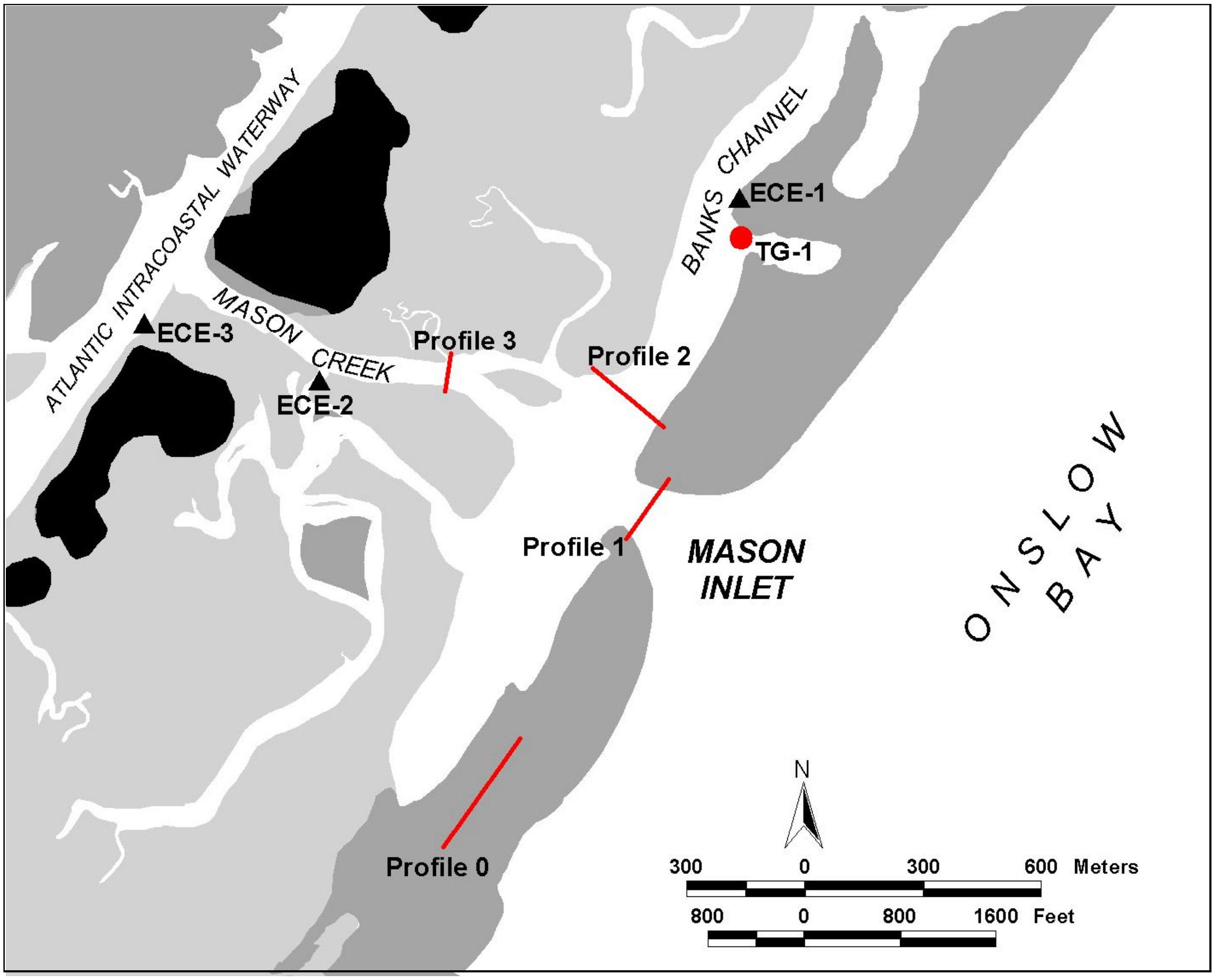

Figure 3. Post-relocation map depicting positions of ADCP transects, photographic baselines, bathymetric profiles, and water-level meters (TG-1). Profile 0 depicts the location of the inlet throat pre-relocation. ECE indicates the location of Erickson Consulting Engineers, Inc., instrumentation.

collaborative efforts of Erickson Consulting Engineers and the USACE for monitoring current velocities and water-level elevations within the estuary behind the inlet. The aforementioned group utilized three stationary, pole-mounted SonTek® Argonaut-SL™ (side-looking) current meters for long-term deployment (months). USACE/ECE instrumentation was located within Banks Channel, Mason Creek, and the AIWW (see Figure 3) and collected current velocities perpendicular to flow and water-level elevations at six-minute intervals while storing the data internally. Instrumentation was referenced vertically (National Geodetic Vertical Datum 1929 (NGVD 29)) and data were combined with numerical models to estimate discharge. Whereas, for the purposes of this study, a vessel-mounted ADCP was utilized during short-term deployments (e.g. 7–14 hour periods) for measuring flow velocities and direction, cross-sectional area, water levels, and calculating discharge and flow volume. The inlet throat (Profile 1) was perceived as an extremely important location for data collection because a majority of inlet parameter relationships rely on throat measurements.

The RD Instruments® ADCP used in this study maintained the capability of being moored at a fixed position on a channel floor in order to gather continuous data (at a fixed time interval) similar to the technique utilized by the USACE/ECE group. However, vessel-mounting the instrument proved to be vastly more advantageous for the purposes of this study. Most importantly, a single ADCP was available for the extensive monitoring that was planned throughout the entire system during a particular survey and consequently needed to be portable. The inherent risk to the instrument was perceived as too great when considering the extremely shallow nature (10 to 14 feet) of the inlet throat and the large volume of boat traffic that the inlet would experience during the study period. Another concern was the migratory nature of the inlet and the eventual burial and perhaps loss of the instrument if the ADCP was moored on the ebb channel floor.

Initial ADCP surveys were limited to the inlet's throat (Profile 1) and were later expanded to include the primary feeder channels, Banks Channel (Profile 2) and Mason Creek (Profile 3) (Figure 3). These surveys were centered on obtaining detailed flow data spanning one-half (12 hr 25 min) and one-quarter (6 hr 12.5 min) tidal cycles. The first two surveys captured one-half tidal cycles, while the remaining six surveys captured one-quarter tidal cycles. Variations in the tidal prism and cross-sectional area were obtained at the inlet throat. These variations are important for characterizing the inlet's hydrographic nature. The primary feeder channels were surveyed in order to gain an understanding of flow distribution through the inlet system. Typical surveys included traversing each channel profile a minimum of four times every half hour from the onset of the survey until completion of the tidal stage of concern.

Each survey was conducted under varying fluctuations in tidal amplitude. However, surveys were conducted during periods when the predicted flood tidal range approximated the measured mean Spring flood tidal range of 4.00 ft. An emphasis was placed on measuring the flood duration of the tide in order to determine the tidal prism for a particular survey. Consequently, seven of the eight surveys included data collection during a flood tide resulting in seven tidal prism values being calculated from flow data collected by the ADCP over the study period.

The ADCP directly measures channel parameters such as flow velocity, direction of flow, water levels, and depth. RD Instruments'® WinRiver™ software was used for the collection of all flow data. WinRiver™ calculated discharge in real-time and cross-sectional area as each profile was traversed across the channel (RDI, 2003). Summary files output by WinRiver™

allowed for further manipulation and post-processing of the flow data within Microsoft® Excel™. Calculated discharge data collected at each profile for the entire cross-section of a channel was manipulated to determine a mean discharge value for each half hour period of an individual field survey. The volume of water that flowed through a channel each half hour was estimated by multiplying 1,800 seconds with the corresponding mean discharge value. Duration of a flood tide was determined from flow speed and directional data. All calculated half hour volume values within a flood tide were then summed to calculate a total volume. This total volume is known also as tidal prism (T_P).

Tidal prism, for the purposes of this study, is defined as the volume of water that enters an inlet on a spring flood tide (USACE, 2003), and cross-sectional area is the channel section under mean tide level (MTL) as determined with the ADCP.

Although the ADCP provides a relatively recent innovation in tidal inlet research data collection, several limitations associated with the instrument and data collection must be addressed. Shallow portions of a channel limit the measurements collected by the ADCP because the instrument cannot consistently measure flow in depths usually encountered along the channel banks (RDI, 2003). Figure 4 depicts the central portion of a channel that is directly measured by the ADCP and the surrounding subsections that cannot be directly measured across a profile. These unmeasured subsections are not unique to the ADCP used in this study but are universal with the use of ADCP's because the limitations are rooted in the technology of the instrumentation. Consequently, WinRiver™ interpolates the discharge through these unmeasured subsections based on data gathered in the central measured section. Another limitation is the ADCP's inability to measure flow when the conditions are such that the channel's bedload is moving. Basically, the ADCP measures flow speed by determining the

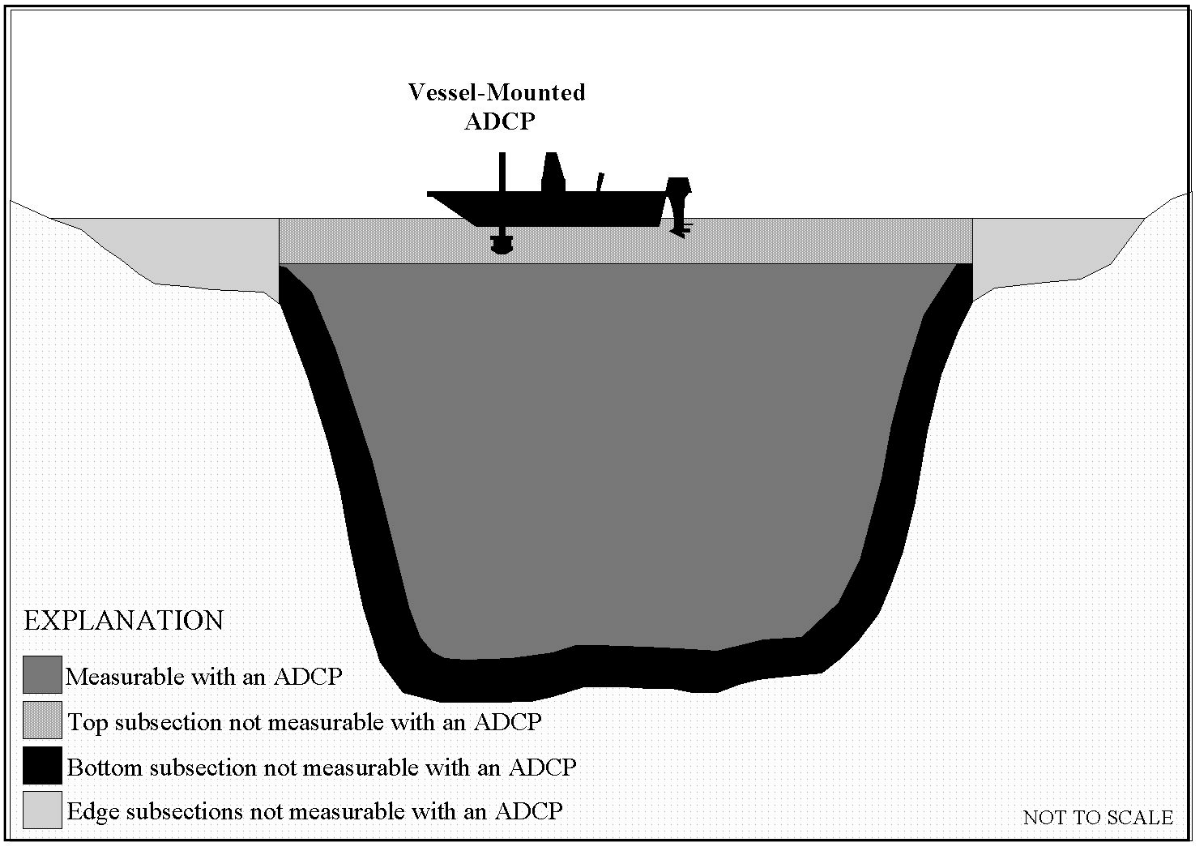

Figure 4. Sketch illustrating the subsections of a channel measured and not measured by an ADCP.

doppler shift associated with transmitting sound at a fixed frequency and receiving echoes returning from sound scatters (e.g. sediment and plankton) in the water column. When the channel floor is moving the doppler shift is affected and creates a situation where the ADCP may over or underestimate flow speed. WinRiver™ informs the user if such a scenario exists and allows for the integration of a depth sounder and GPS in addition to the ADCP. A depth sounder is able to "hear" the true bottom while penetrating through the moving sediment whereas the GPS informs the ADCP as to where in space it is located. Combining these instruments with an ADCP allows for the measurement of flow under fast moving, turbid conditions.

Specific commands necessary for input into the ADCP depended on site-specific conditions of the inlet system, which included: maximum depth, salinity, water temperature, tranquil or turbid flow conditions, suspended sediment concentrations, and channel bedload characteristics. The Configuration Wizard within WinRiver's™ acquire mode allowed the user to define the parameters of the study area and define thecommands sent to the ADCP for the inlet system. A compass calibration was performed upon the ADCP in order to correct for local magnetic variation and for one-cycle magnetic deviation errors induced by ferrous objects (e.g. motor) near the ADCP. All ADCP data were collected in Water Profiling Mode 1, which was recommended for fast flow conditions of any depth with rough and dynamic situations. Due to the dynamic nature of the system modification to certain commands were performed if needed during a survey. All default commands (set by RDI) were used in configuration of the ADCP except for commands controlling depth cell size and number, blanking distance, salinity, and time between pings. Depth cell size and blanking distance were set to 0.82 ft, whereas depth cell number was dependent on depth, time between pings was set to 0.09 seconds, and the salinity was set for 35 ppt. The Power Method, within WinRiver™, estimated discharge measurements for both the unmeasured top and bottom portions of the channel profile. Power extrapolation fits a power curve to the directly measured section of the water profile, and then uses this power law fit combined with Chen's coefficient (0.1667) to compute the discharge in the unmeasured top and bottom subsections (RDI, 2003). Edge estimates of discharge along both shoulder margins were determined with the assumption that a triangular area shape existed between the final good ensemble and the channel bank edge. A ratio-interpolation method was used for estimating the velocity between the channel bank and the last known mean velocity determined by averaging water velocity in several ensembles.

Sources of error in the measured subsections include ADCP instrument error and flow variations through the inlet. MORLOCK (1996) determined that discharges in the top and bottom subsections are extrapolated from the measured subsections, resulting in discharge errors of similar magnitude for these estimated subsections. Based on the error equations for discharge measurement presented in MORLOCK's (1996) paper, it was determined within the throat under a worst-case scenario that a total error of approximately 3% existed for this particular inlet. ADCP instrument error for the measured channel subsection was determined to be 11.6 ft^3/s, whereas top, bottom, and opposing southwest/northeast edge subsection errors were 14.9 ft^3/s, 2.2 ft^3/s, 8.8 ft^3/s and 146.5 ft^3/s, respectively.

Ebb-Tidal Delta and Inlet Throat Topo-Bathymetric Analyses

Topo-bathymetric data collected by GBA was used in the measurement of throat parameters and volumetric analyses of the system. GBA surveys covered an area encompassing the tidal creeks feeding the inlet, the main ebb channel, the shoreface updrift and downdrift of the inlet, and the ebb-tidal delta region offshore of the inlet. These data were initially referenced to the vertical datum NGVD 29 and were converted to NAVD 88 with a conversion offset of -0.95 ft for New Hanover County (National Flood Insurance Program, 2003).

ESRI® ArcView™ GIS version 3.2 software was used to manipulate and display the referenced data. An extension of ArcView™, known as 3D Analyst™, allowed for the generation of digital terrain models known as triangulated irregular networks (TINs) based on these data. A TIN is used to represent a surface using contiguous, non-overlapping triangles. TINs are used for detailed, large-scale applications and were considered optimal for the purposes of this study. BYRNES *et al*. (2002) recommends that the TIN method be used for the creation of accurate model surfaces from topo-bathymetric data for calculating volume change and determining sediment transport patterns. A total of six topo-bathymetric data sets surveyed by GBA between March 2002 and October 2003 were supplied for analyses. Each data set was used for the generation of a TIN model and a corresponding topo-bathymetric map of the study area to be used in laboratory analyses. The March 2002 survey was completed between the 7th and 14th, the period between the new inlet's opening and the old inlet's closure, yet failed to measure the intertidal beach between the +4 ft and -6 ft contours 1,500 ft northeast and 1,700 ft southwest of the new inlet.

Measurements from these models, taken for the purpose of this study, focused on two main regions of the study area, the new ebb-tidal delta and the inlet throat. Profiles across the inlet throat were generated for each survey along Profile 1 to determine the channel's cross-sectional area, aspect ratio (width:depth), and wetted perimeter (Figure 3). Cross-sectional area, channel width, and depth along Profile 1 were all measured at or below MSL (-0.31 ft). Wetted perimeter (W_P) refers to the portion of the throat cross-sectional area's perimeter that makes contact with the channel's opposing banks and floor below MSL.

Several studies describe a methodology for calculating the ebb-tidal delta volume by reference to idealized no-inlet bathymetric lines (DEAN and WALTON, 1975; WALTON and ADAMS, 1976; MARINO, 1986; STAUBLE, 1998). HICKS and HUME (1996) developed the residual method for analyses of ebb shoal shapes and volumes. In order to perform calculations on the ebb-tidal delta's volume, it is critical to define the boundary of the ebb shoal. Unfortunately, standardized techniques to determine these boundaries do not exist (STAUBLE, 1998). Volume of the evolving ebb shoal was determined using a variation of the method described by DEAN and WALTON (1975) for estimating quantities of sand stored in outer shoals of inlets on sandy coasts. The method used for this study was similar to STAUBLE's (1998) Residual Method.

The March 2002 bathymetric map of the inlet's offshore region was utilized to construct an idealized no-inlet condition by assuming that the natural shape of the coast would mimic the parallel bathymetric lines updrift and downdrift of the inlet. Bathymetric lines of a common depth updrift and downdrift were then joined to follow the general parallel of the shoreline only in areas where field measurements were not obtained. An idealized "No-inlet" TIN was created based on this no-inlet bathymetric map and was used as a base-line surface from which all ebb shoal volumes were calculated. Utilizing the bathymetric maps created from each study area TIN, a delineation of the ebb shoal's boundary was determined in the offshore region, allowing for the creation of a unique ebb-tidal delta TIN for each survey completed. For the purposes of this study, the boundary of an ebb shoal included a landward baseline across the inlet's mouth, the updrift and downdrift shorelines, the seaward-most bathymetric line affected by the inlet, and the inflection points updrift and downdrift of the inlet. The 3D Analyst™ extension allowed each unique ebb delta TIN to be superimposed upon the "No-inlet" TIN in order for a cut-and-fill analysis to be performed. The cut-and-fill analysis generates a new residual map depicting areas within the ebb shoal's boundary that either lost or gained material based on the "No-inlet" surface. The volume gained within this area was considered to be the volume of the ebb shoal for a particular survey. This was the volume of material found above the March 2002 surface.

Flood Shoal

A short-term, six week monitoring study to track the migration rate and volumetric changes on the subaerial portion of a migrating sand shoal within Banks Channel was conducted during low tide conditions (Figure 5). The monitoring period lasted six weeks to effectively span a full lunar month and to ascertain the effects of both Spring and Neap tides on sediment transport within this section of the inlet system. Topo-bathymetric data were obtained with a Trimble® 5700 RTK-GPS system with surveys conducted once during each week of the study period. This instrumentation allows for the precise measurement of points upon the Earth's surface that can be referenced to a variety of vertical datums and horizontal coordinate systems. All data were referenced vertically to NAVD 88 and horizontally to North Carolina State Plane 1983. A fixed grid consisting of thirty transects was established in order to survey a constant area (118,000 ft^2) of the shoal each week. This portion of shoal was mapped by walking and taking measurements every 2 feet along each transect.

All topo-bathymetric data were entered into ArcView™ 3.2 and manipulated with the 3D Analyst™ extension. The TIN surfaces with corresponding topo-bathymetric maps were generated from the collected data from each field survey. The 3D Analyst™ extension allows the user to select a specific contour on a surface from which a volume can be determined above or below. An arbitrary base elevation of -3.58 ft was selected in order to compute the shoal

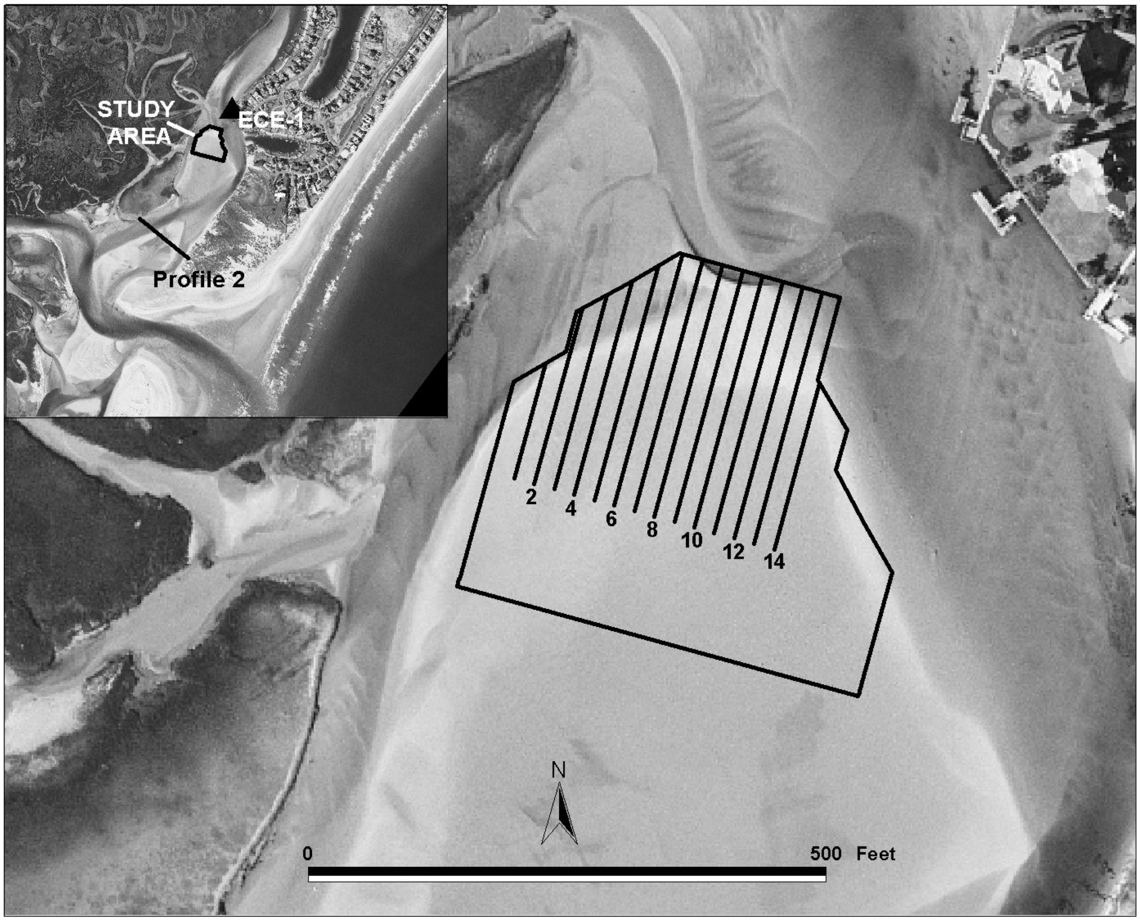

Figure 5. Vertical aerial photograph showing the Banks Channel flood shoal complex. The outlined area indicates the study area, whereas the numbered lines are the transects used to measure migration of the shoal.

volume above this plane and below a TIN's surface. This elevation was chosen because it was the lowest elevation mapped consistently with the RTK-GPS. It should be noted that GBA collected topo-bathymetric data over the same shoal area. However, the spacing of their measurements was too great to derive anadequate estimation of volume change and bedform migration on this particular portion of the shoal. A cut-and-fill analysis was performed using this extension in order to check the validity of the volume estimates. Cut-and-fill analysis determines how much material has been lost or gained in a study area by comparing two digital terrain models of the area, one before a change and one after.

Using the topo-bathymetric maps a unique bedform feature (-0.58-foot contour) was selected as a marker to track the migration of the shoal. This contour was chosen because it closely approximated the shape of the bedform and was consistently mapped during the study period. A series of fourteen transects, directed along a northeastern orientation, was established across this feature (Figure 5). Utilizing another extension of ArcView™, Simple Change Analysis of Retrograding and Prograding Systems (SCARPS) version 2.04, the migration rates and position changes of this feature along each transect was determined (JACKSON, 2004).

Vertical Aerial Photographs

Eleven sets of vertical aerial photographs were selected, from various agencies, dating both prior to and following the relocation of the inlet in order to track changes in inlet position, opposing shoulder positions, inlet width, ebb channel orientation, and shoreline position along portions of Figure Eight Island and Wrightsville Beach (Table 1). These aerial photographs were partitioned to define a pre-relocation period (February 1998 to February 2002) and a post-relocation period (May 2002 to October 2003) for shoreline change analyses. A different post-

Table 1. List of vertical aerial photographic sets, associated agencies, scale and error.

Vertical Aerial Photographic Sets			
Date	Source	Scale	Average Error (ft)
17-Feb-98	New Hanover County	1:12,000	2.15
19-Jun-98	NCDENR	1:12,000	Base Layer
11-Oct-00	U.S. Army Corps of Engineers	1:12,000	2.96
20-Feb-02	U.S. Army Corps of Engineers	1:12,000	3.31
16-May-02	U.S. Army Corps of Engineers	1:12,000	3.98
01-Aug-02	Gahagan & Bryant Associates, Inc.	1:12,000	1.84
14-Nov-02	Gahagan & Bryant Associates, Inc.	1:12,000	1.06
15-Jan-03	Gahagan & Bryant Associates, Inc.	1:12,000	2.10
10-Mar-03	U.S. Army Corps of Engineers	1:12,000	3.70
11-May-03	Gahagan & Bryant Associates, Inc.	1:12,000	1.86
31-Oct-03	Gahagan & Bryant Associates, Inc.	1:12,000	1.81

relocation period (March 2002 to October 2003), with utilization of topo-bathymetric data gathered in March 2002, was generated to track changes in inlet width, channel orientation, and position of the ebb channel and shoulder margins. Reasoning behind the formulation of two separate post-relocation periods was rooted in the incomplete data set for the March (As-built) 2002 survey. Topo-bathymetric data was lacking along the shoreline reaches 1,500 ft northeast and 1,700 ft southwest of the new inlet, however it included coverage of the excavated inlet channel. Although combining different data sets is generally not advised, the March 2002 topo-bathymetric data was included in an effort to generate a more robust data set and gain a better understanding of the immediate changes near the inlet channel.

GBA supplied rectified aerials with a 1.0-ft/pixel image resolution and required minimal manipulation prior to digitization. The North Carolina Division of Coastal Management (NCDCM) performed orthorectification on photographs obtained from the Department of Transportation along this section of coastline yielding an image resolution of 0.5-ft/pixel. USACE aerial photographs were scanned at 600 dpi (resulting in a 1.6-ft/pixel image) and exported as uncompressed TIFF images. Simple rectification of these photographic sets within ArcView™ required a bilinear registration (2nd order polynomial), geo-referencing to a base layer of 1998 digital orthophotos (NCDENR) in North Carolina State Plane 1983 coordinate system, and at least 10 to 15 ground control points per photograph.

The target average root-mean-square (RMSE) value for each of these photographs remained below 15 ft of error. RMSE values are listed in Table 1 and represent the average error for each rectified photograph set. The high-water line (HWL) was selected as the primary reference of shoreline position (DOLAN *et al*., 1978, 1980; PAJAK and LEATHERMAN, 2002). However, shoreline position errors include an amalgam of incorporated errors in photographic quality, operator dexterity, and digitizing techniques. Previous work has determined worst-case error estimates for rectified aerial photography at approximately 25 ft (CROWELL *et al*., 1991). Error comprising this worst-case total included: distortion of air photos (3–7 ft of error), error delineation of the HWL from good quality air photographs (<16 ft), digitizer error (<1 ft), and digitizer-operator error (~8 ft).

Inlet width was measured between the opposing digitized shorelines for all photographic sets and along respective profiles delineated for the pre- (February 1998 to February 2002) and post-relocation (March 2002 to October 2003) periods. A contour map of the March (As-built) 2002 topo-bathymetric data allowed for the measurement of inlet width between the 2-ft contours located on opposing shoulders. The fixed pre- (Profile 0) and post-relocation (Profile 1) alongshore baselines approximate the position of the inlet's minimum width, the migration trend direction, and follow the general orientation of the coast for each period (Figure 3).

Inlet position was determined for each photograph and the March 2002 topo-bathymetric data set by measuring the distance, along Profile 0 and Profile 1, from an arbitrary reference point to the center of the main ebb channel. Opposing shoulder positions, located on Figure Eight Island and Wrightsville Beach, along these baselines were also measured in the same manner. Positions were converted such that they refer to the position of the main ebb channel or respective shoulder margin on the February 1998 photograph and March 2002 topo-bathymetric map, which represent the initial positions for the pre- and post-relocation periods, respectively.

Shoreline position was determined by delineation of the HWL along the southern end of Figure Eight Island and the northern end of Wrightsville Beach. An offshore baseline paralleling the coastline was erected and used to launch a series of thirty landward transects spaced at an interval of 400 ft while encompassing the inlet relocation zone and a 2.2-mile stretch along the coast (Figure 6). The SCARPS extension of ArcView™ allowed for determination of shoreline change and migration rates for the periods prior to and post-relocation. All shoreline positions and rates were based on the initial data sets (February 1998 and May 2002) for the pre- and post-relocation periods. Various rates generated by SCARPS include the end point rate (EPR), linear regression rate (LRR), and average of end point rates (AER). For purposes of this study the EPR, commonly known as the net migration rate, was determined to effectively represent the migratory patterns of this system and consequently used for comparative purposes. Shoreline change trends were determined for the periods preceding and following inlet relocation. Net shoreline change refers to a positional change experienced between two shorelines; in contrast, cumulative shoreline change utilizes all shoreline positional changes instead of only two within a set period of time.

Correlation coefficients (Pearson-r, henceforth termed r) were calculated between inlet width and channel position, and cumulative inlet migration and cumulative shoreline change, and other parameters. Thus, possible relationships between these parameters were defined.

RESULTS

Water-Level Data

Data gathered from TG-1 in Banks Channel was used to determine tidal parameters such as MSL, durations, and ranges (Figure 3). Mean sea level was determined to exist at an elevation of -0.31 ft (NAVD 88) whereas mean high water and mean low water were 1.33 ft and -1.95 ft, respectively. Tidal ranges and durations under various tidal conditions are presented in Table 2.

Based on the classification scheme devised by HAYES (1979) and the measured mean tidal range of 3.28 ft, Mason Inlet falls within the extreme upper limit of the microtidal category.

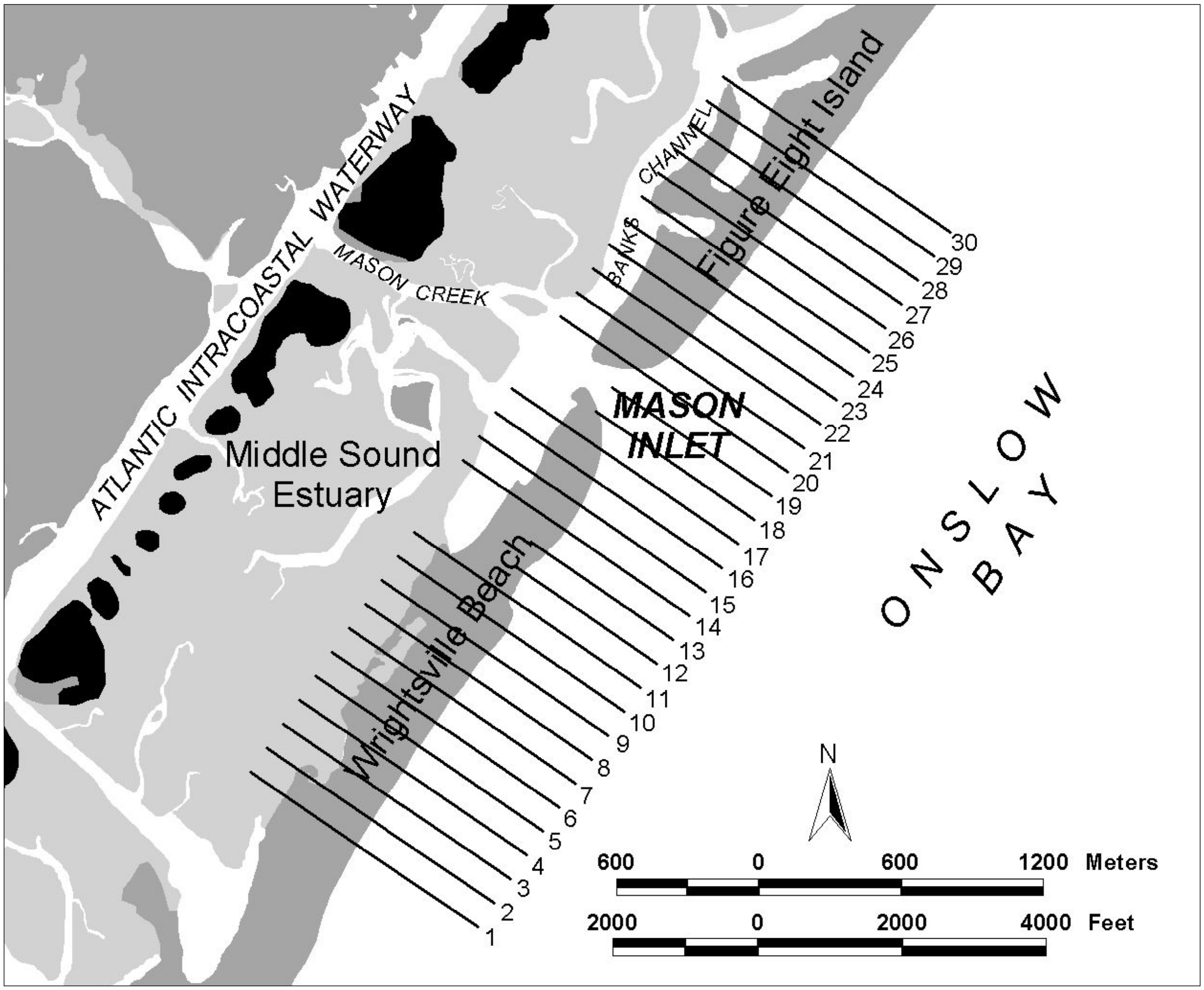

Figure 6. Post-relocation map depicting shoreline transects (400-ft spacing) along Figure Eight Island and Wrightsville Beach.

Table 2. List of tidal data obtained from TG-1 located in Banks Channel.

Tidal Parameters	Mean Range (ft)	Mean Duration (hrs)
All Data	3.28	6.21
Flood Tide	3.28	5.84
Ebb Tide	3.28	6.59
Spring Flood Tide	3.95	5.61
Spring Ebb Tide	3.91	6.78
Neap Flood Tide	2.63	5.68
Neap Ebb Tide	2.69	6.78

Determination of mean flood duration (5.84 hr), based on water level readings, was found to be considerably shorter than the mean ebb duration (6.59 hr). Focusing on the Spring tidal phase, a similar trend occurred with the mean ebb duration lasting 1.17 hours longer than the mean flood duration (5.61 hr). As a final verification, the Neap tidal phase revealed a shorter mean flood duration of 5.68 hr when compared with the mean ebb duration of 6.78 hr.

Vertical Aerial Photographic Data

Inlet Dimensional Data

Inspection of photographs revealed that a measurable degree of morphologic variability occurred within the inlet throat over the four-year period before relocation (Figure 7). Emplacement of sandbags and geo-tubes along the southern margin of the inlet in 1997 stabilized the ebb channel and inlet throat, allowing for the width and cross-sectional area to adjust accordingly. Between 1998 and 2000, 112 ft of continued elongation of the updrift spit due to migration reduced the inlet width from 1,122 to 1,012 ft. The net southwest elongation of the updrift spit during this four-year period was 341 ft. As a direct result of encroachment by the northern margin of the inlet and readjustment of shoals in the main feeder channel, the length of Banks Channel increased thereby lengthening the flushing distance between the inlet throat and the AIWW from 16,994 ft to 17,643 ft. Also during this period, noticeable movement and accumulation of sand within the inlet throat was noted. Immediately prior to relocation (February 2002) inlet width measured 788 ft and the ebb channel floor had shoaled to a depth of -9.3 ft (NAVD 88).

Shoal complexes comprising the flood and ebb-tidal deltas also experienced morphologic changes that specifically relate to the variability within the inlet throat. Specifically, the shoal

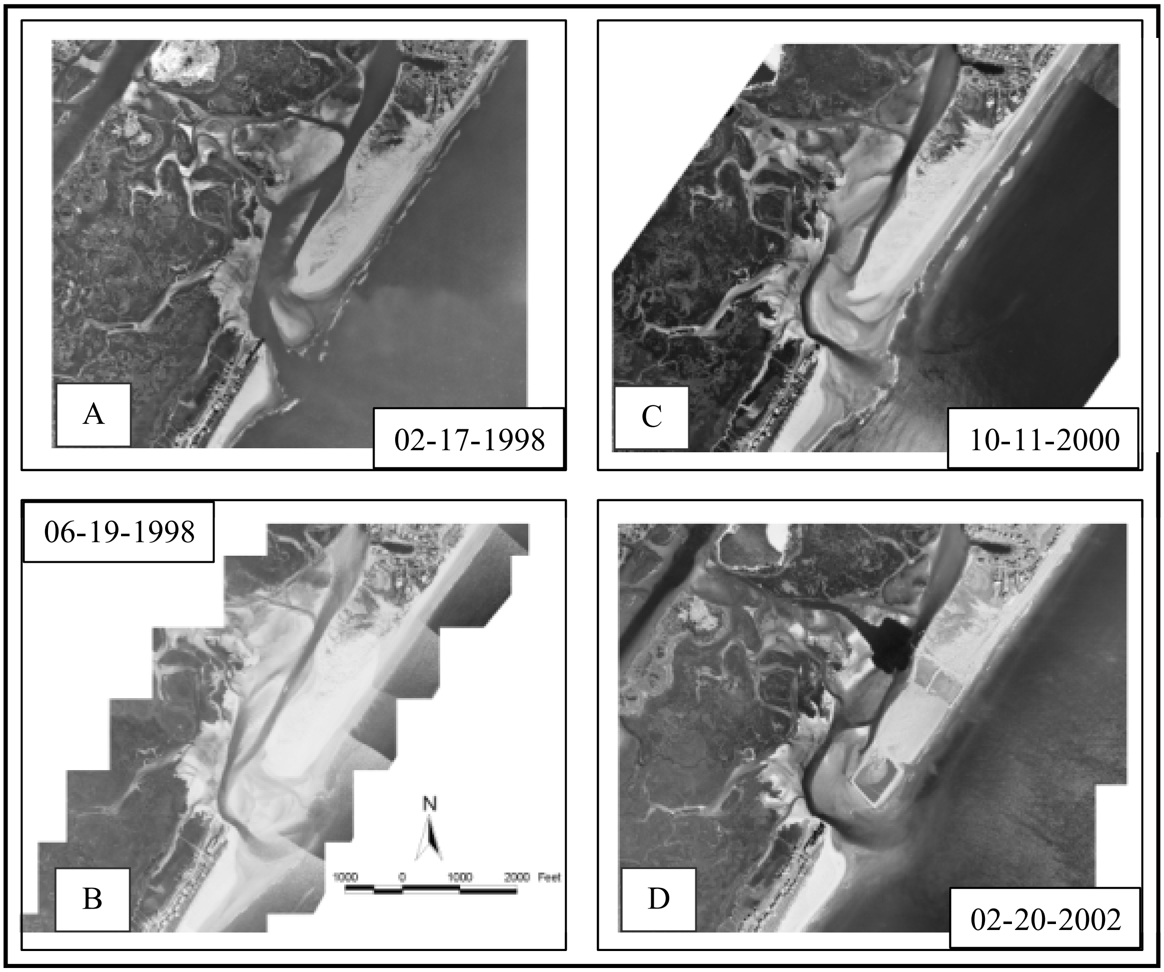

Figure 7. Aerial photographs illustrating the shoaling trend within the feeder channels prior to relocation of the inlet. Note that scale is consistent for each photograph.

of the ebb-tidal delta, defined on photographs by waves breaking around the perimeter of the shoal, experienced a 17% decrease in area after the bags were emplaced until the onset of the relocation project. Conversely, increases in sedimentation of the feeder channels and on the flood-tidal delta were particularly noticeable within the primary feeder channel of Banks Channel. The formation of large, well-developed shoal complexes accumulated predominantly within this channel and efficiently plugged Banks Channel over time. Throughout this period, Mason Creek was shoaled and considered unnavigable leaving Banks Channel as the only viable corridor between the waterway and ocean (Figure 7).

Examination of Figure 8 suggests that the feeder channels of the system continued to experience a high degree of sedimentation after relocation. Based on Figure 8, the shoaling nature is quite evident. The sedimentation basin, Banks Channel, and Mason Creek along with its intersection at the AIWW, all became choked with sediment within one year following the relocation project. Well-developed lobes of the flood-tidal delta can be observed extending within Banks Channel both north and south of the inlet's main ebb channel with lesser amounts of sediment developing point bars within Mason Creek. The development of two unique lobes within the portion of Banks Channel behind Figure Eight Island can be seen in Figure 8b where the lower portion of the channel was bifurcated into two separate connections with the main ebb channel. Spit development off Figure Eight's southern terminus resulted in coalescence of a lobe of the flood-tidal delta with the spit while forming one predominant channel within Banks Channel (Figure 8c and 8d).

Net Shoreline Change

Measurements focusing on net shoreline changes before (February 1998 to February 2002) and after the relocation (May 2002 to October 2003) indicated opposing accretion/erosion

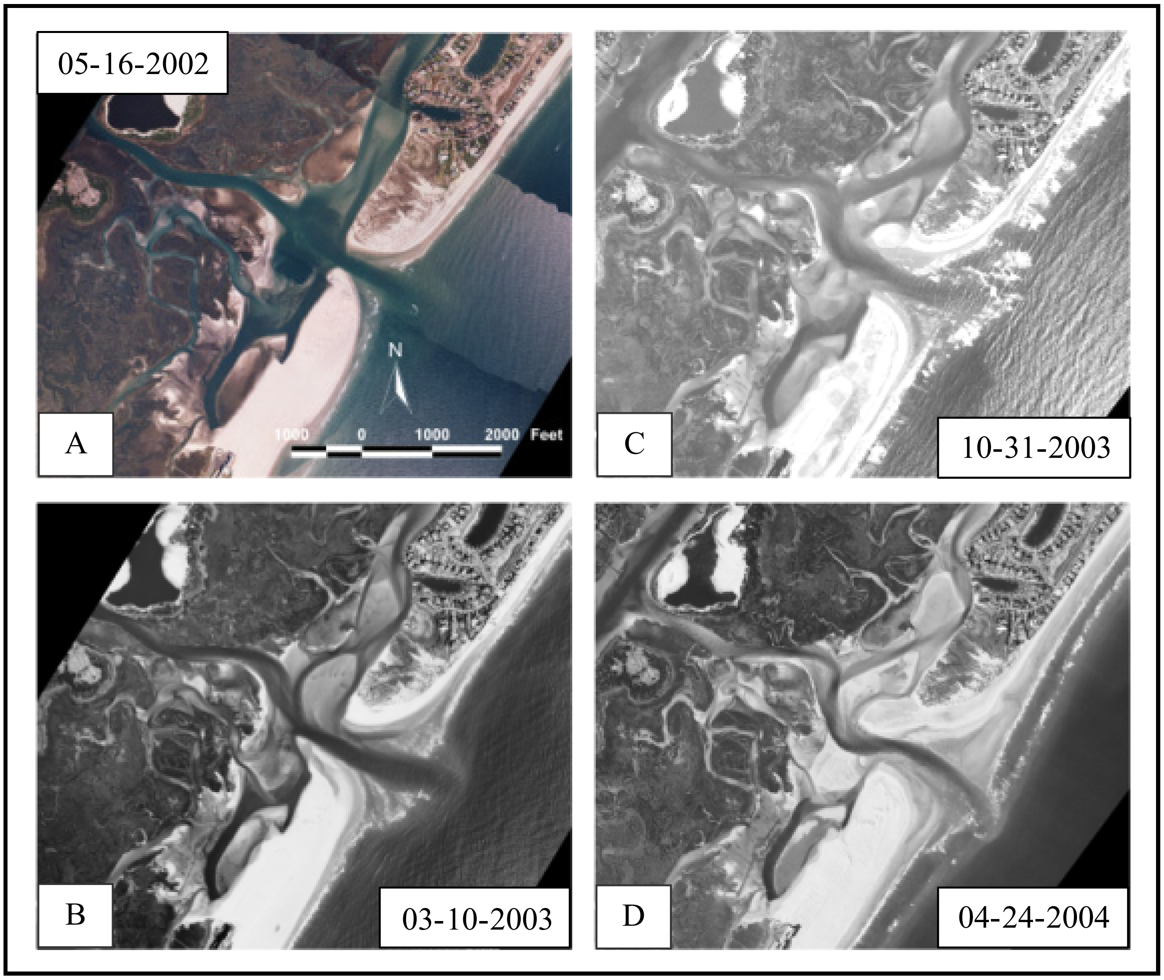

Figure 8. Photographic set depicting a continued shoaling trend within the feeder channels after relocation of the inlet.

trends at 20 of the 28 transects along the 11,600-ft coastal segment of concern (Figures 6 and 9). Although 30 transects were positioned along the 11,600-ft coastal segment monitored in this study, only 28 transects during the pre/post-relocation periods actually measured shoreline change. These gaps in the shoreline position data are attributed to the locations of the inlet channel prior to (Transects 12 and 13) and after relocation (Transects 18 and 19) where the shoreline was nonexistent. Overall, between 1998 and 2002, this segment experienced net accretion with erosion occurring at Transects 11 and 15 on the immediately opposing flanks of the inlet (Figure 9). Net accretion was measured on all other transects except, Transects 12 and 13, where the original inlet channel and swash platform existed.

Relocation of the inlet resulted in a distinct adjustment to the planform of the neighboring islands. A majority of the shoreline (22 of 28 transects) experienced net erosion (ranging from 6 ft to 549 ft of erosion) between May 2002 and October 2003 (Figure 9). Transects 11–13 were positioned within the original inlet zone resulting in an accretionary event of between 23–114 ft of shoreline progradation along this small segment as the old ebb shoal collapsed alongshore. The "shoreline bump" (Figure 10), seaward of the resort complex situated within Transects 4–10, experienced between 24–115 ft of erosion as the shoreline sought to assume a more uniform orientation in alignment with the new inlet conditions. Erosion along the 1,600-ft long downdrift segment (ranging from 6–549 ft) and along the 4,400-ft long updrift segment (ranging from 74–140 ft) that flank the new inlet generally diminished with distance from the inlet.

Pre- and Post-Relocation Comparisons and Relationships

Mason Inlet's preliminary evolution, in terms of width and position, is presented in Figure 11a. Position of the inlet refers to the intersection of the ebb channel's centerline with

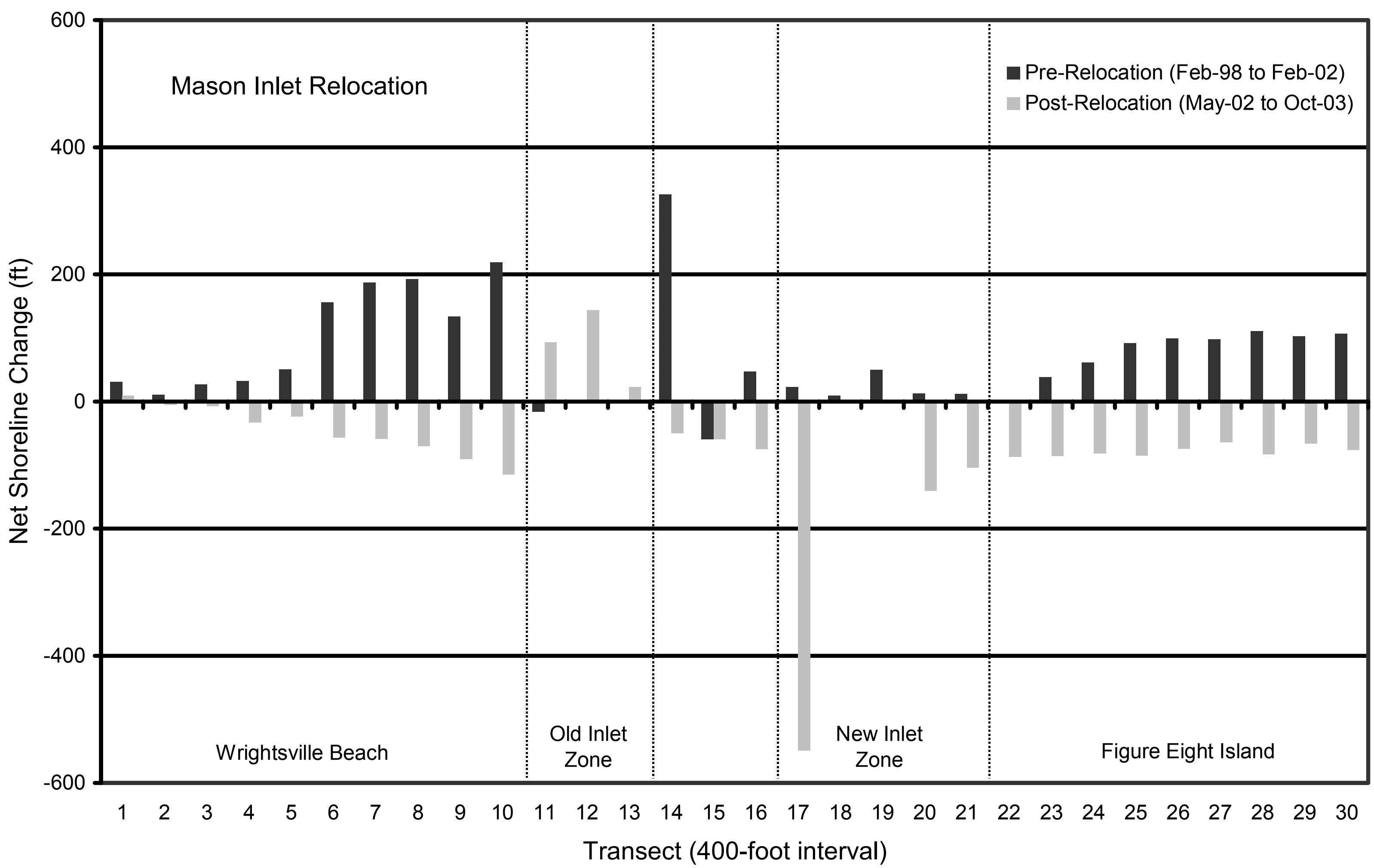

Figure 9. Graph depicting the net shoreline change before and after relocation of the inlet. Positive values are indicative of net accretion whereas negative values are indicative of net erosion at an individual transect.

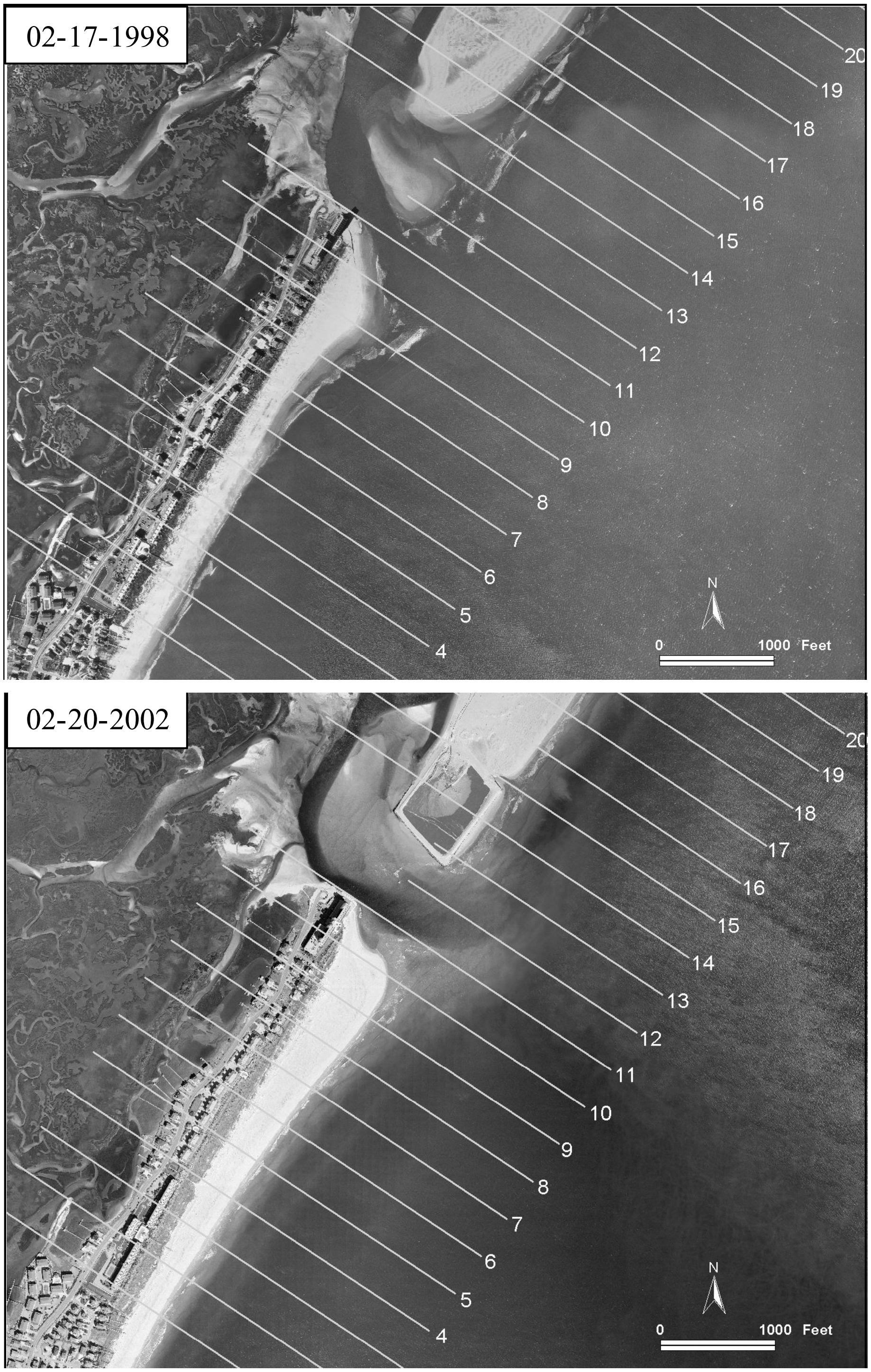

Figure 10. Aerial photographs depicting the "shoreline bump" situated within Transects 4–10 along the northern portion of Wrightsville Beach. Notice growth of the feature during the four years prior to the relocation.

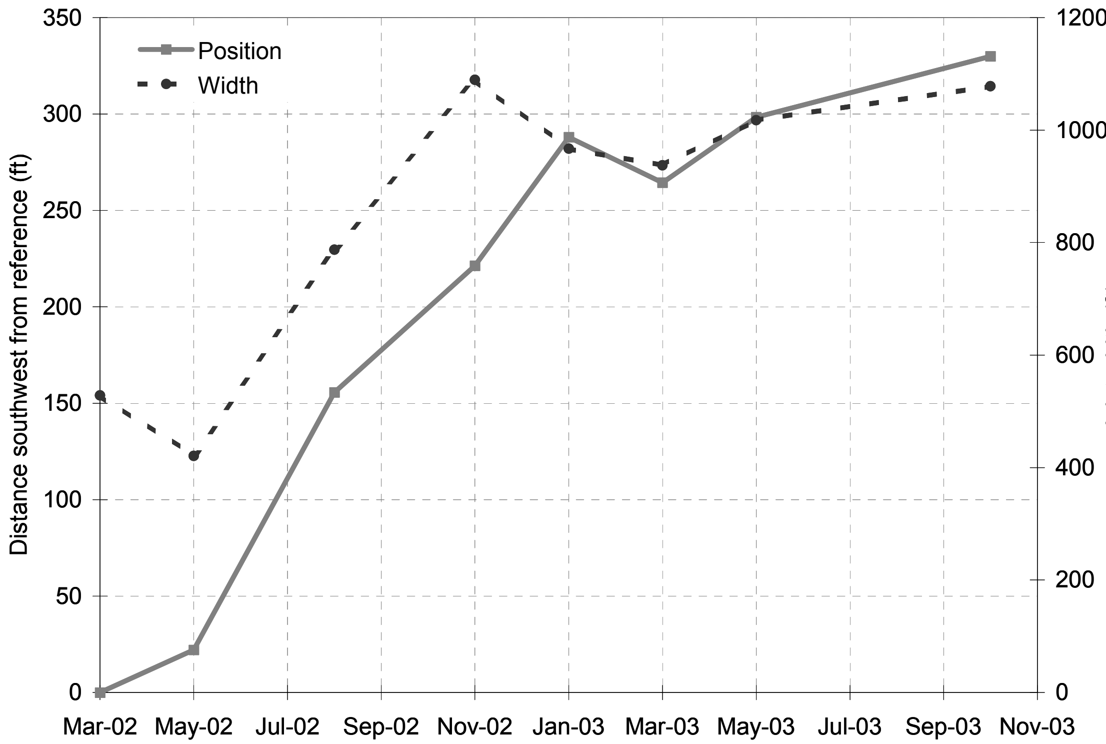

A

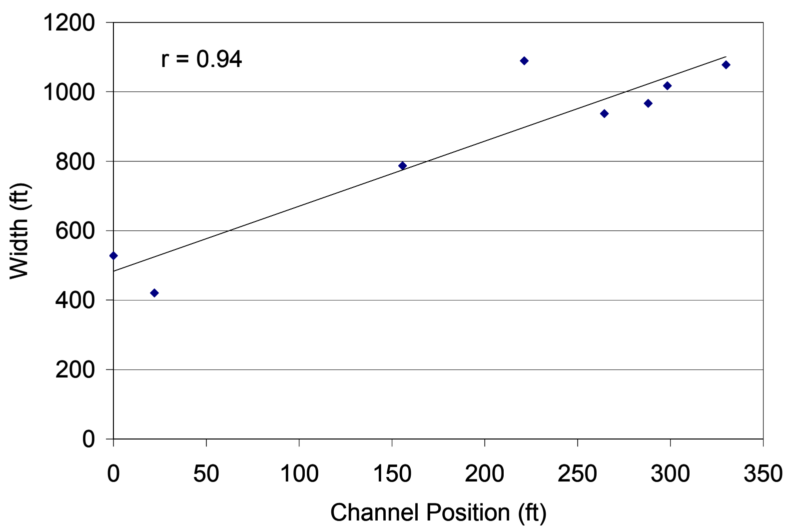

B

Figure 11. (a) Graph illustrating inlet width and migration distance since the opening of the inlet. The reference point refers to the position of the ebb channel when the inlet was opened on March 7, 2002. (b) Graph depicting the high correlation between inlet channel position and width following the relocation.

Profile 0 (pre-relocation period) or Profile 1 (post-relocation period) (see Figure 3). Excavation of the new inlet created an artificial channel width of approximately 528 ft upon opening of the inlet in March 2002. An initial adjustment of the inlet caused a subsequent reduction in width to 421 ft by May 2002. Extensive widening of the inlet occurred (668 ft) during a six-month period between May and November of 2002 when the width reached its maximum of 1,089 ft. Following this period, variations in inlet width were diminished reaching a minimum value of 937 ft in May 2003 and measuring 1,078 ft by the end of the study in October 2003. Mean inlet width for this eleven-month period was 1,018 ft and compares closely to the mean inlet width of 1,030 ft measured for the pre-relocation period.

Comparison of the positional changes and EPR's (migration rates) of the Figure Eight Island shoulder, Wrightsville Beach shoulder, and inlet's ebb channel over the duration of the study revealed large contrasts between the pre- and post-relocation periods (Table 3). Although the overall migration trend in the southwesterly direction (positive values) continued after relocation, the migration rates varied greatly from those measured prior to the relocation effort. The average of end point rates (AER) calculated for the pre-relocation period (February 1998 to February 2002) was determined to be 125 ft/yr while the corresponding value during the post-relocation period (May 2002 to October 2003) was 268 ft/yr. After the relocation, maximum net migration rates (net EPR) were measured during the initial stages of inlet evolution to be 387 ft/yr by August 2002 and diminished incrementally to 200 ft/yr by October 2003.

Comparison of inlet width to inlet ebb channel position indicates a relationship during the post- relocation period in particular (Figure 11b). The correlation coefficient between these two parameters is quite high at 0.94 (significant with 99% of confidence). Consequently, channel position and inlet width appear to be related at least during the initial stages of inlet evolution.

Table 3. Migration rates and position changes for the inlet throat, Figure Eight shoulder, and Wrightsville Beach shoulder. Pre-relocation measurements were taken along Profile 0; whereas, post-relocation measurements were along Profile 1 (see Figure 2). Note that positive values represent southwest migration; whereas, negative values are indicative of northeasterly migration of a particular feature.

		EPR (ft/yr) - from preceeding date			*Net EPR (ft/yr)	Position Change (ft) - from preceeding date		
	Date	Figure Eight Shoulder	Wrightsville Beach Shoulder	Ebb Channel	Ebb Channel	Figure Eight Shoulder	Wrightsville Beach Shoulder	Ebb Channel
Pre-Relocation	Feb-98	-	-	-	-	-	-	-
	Jun-98	-201	27	309	309	-67	9	103
	Oct-00	77	-3	-3	37	179	-8	-7
	Feb-02	168	4	15	29	229	5	21
	*Net	85	2	29	-	341	7	117
Post-Relocation	Mar-02	-	-	-	-	-	-	-
	May-02	25	-533	115	115	5	-102	22
	Aug-02	-133	1603	633	387	-28	338	134
	Nov-02	-264	785	228	321	-76	226	66
	Jan-03	733	12	393	335	124	2	67
	Mar-03	287	89	-160	262	43	13	-24
	May-03	-1030	-559	200	253	-175	-95	34
	Oct-03	70	198	67	200	33	94	32
	*Net	-45	288	200	-	-74	476	330

*Net refers to the rate or position change from the initial date to the most current date for both the pre-relocation and post-relocation periods.

Inlet channel position, along with opposing shoulder margin positions measured along Profile 1 (see Figure 3), experienced marked changes during the first 20 months of inlet evolution (Figure 12). Based on the historical nature of the inlet, it was expected that after an initial adjustment period the inlet would begin its southwesterly migration. As expected, within two months of opening the ebb channel had migrated 22 ft and the Figure Eight shoulder had migrated 5 ft to the southwest. The Wrightsville Beach shoulder shifted 102 ft to the northeast during this same period. Following this initial adjustment, the Wrightsville Beach shoulder began its southwesterly migration with a shift of 564 ft between May and November of 2002 with the Figure Eight shoulder exhibiting an opposite trend of 104 ft of movement to the northeast. Variations in the position of these features continued after November 2002 but to a lesser extent with the Wrightsville Beach shoulder reaching its furthest position of 477 ft (March 2003) and its closest position 382 ft (May 2003) southwest from its initial position. During this period the Figure Eight shoulder fluctuated as much as 68 ft south (March 2003) and 107 ft north (May 2003) of its initial position. By January 2003, the ebb channel had reached a position 288 ft southwest of its initial position. Southwest migration of the ebb channel slowed after with only an additional 42 ft of migration by October 2003.

Inlet/Shoreline Relationships

Net trends in shoreline movement, presented previously, aided in the delineation of three shoreline zones for monitoring relationships influenced by the new inlet system (Figure 13). Zone I encompassed Transects 7–16 and the downdrift segment along Wrightsville Beach, while Zone III (Transects 21-30) spanned the updrift shoreline fronting the southern 3,600 feet of

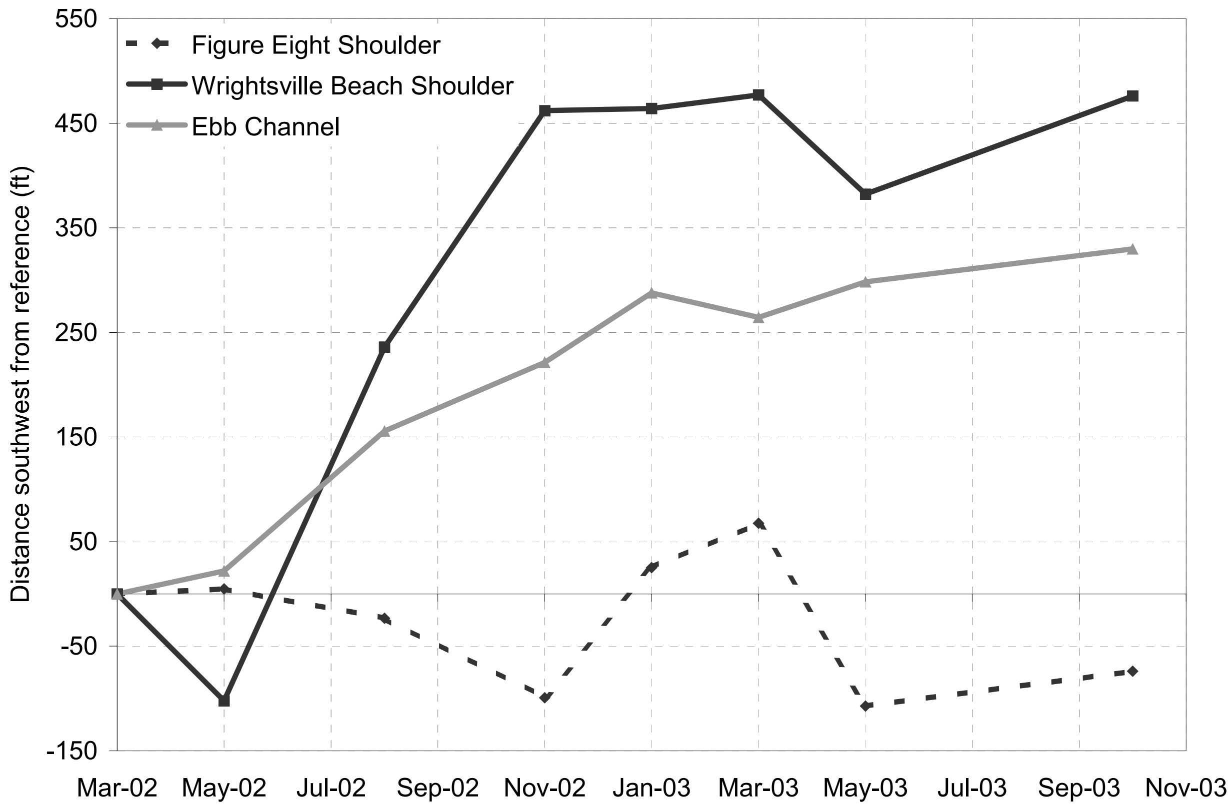

Figure 12. Graph depicting inlet evolution at Profile 1: Position of inlet channel, and both shoulders of the inlet through time. Note that negative values represent positions northeast of the position in March 2002.

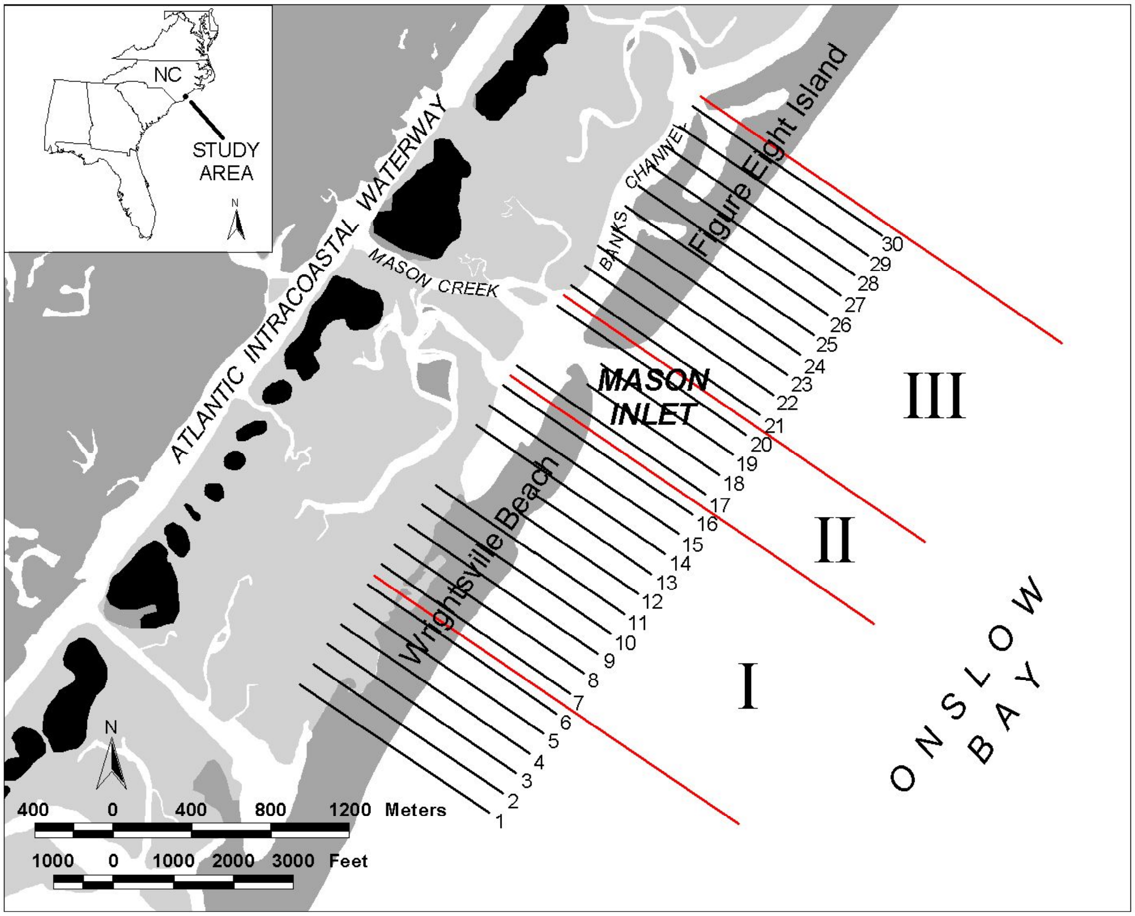

Figure 13. Post-relocation map depicting three delineated shoreline zones. The extended lines represent boundaries between neighboring zones.

Figure Eight Island. Zone II, within Transects 17–20, was the segment directly seaward of inlet throat.

Generation of shoreline reaches for the post-relocation period allowed for the comparison of shoreline change along the neighboring beaches to the migration of the inlet from May 2002 to October 2003. A relationship, specifically during this post-relocation period, existed between inlet channel migration and cumulative shoreline change within Zones I and III. Figure 14 illustrates the relationship between the inlet channel's southwesterly movement and the cumulative erosion experienced along the beaches of Figure Eight Island and Wrightsville Beach. Correlation coefficient values between these parameters are very high, 0.99 for Wrightsville Beach (Zone I) and 0.93 for Figure Eight Island (Zone III). Thus, channel migration and cumulative shoreline change along neighboring oceanfront shorelines appear to be dependent processes for this inlet.

Topo-Bathymetric Data

Channel Cross-Section Changes

The conventional position to measure channel cross-sectional area (A_C) is at the MSL throat section based on the assumption that this is representative of the average section through which tidal volume flows (KANA and MASON, 1988). The large variation in cross-sectional area and channel shape at the inlet throat is depicted in Figure 15. Table 4 lists the survey results for the throat (Profile 1).

During the construction phase of the relocation effort the new inlet channel was excavated to create a cross-section of approximately 4,867 ft^2. The initial adjustment of the inlet during the first four months of evolution is depicted in Figure 15a where the cross-section

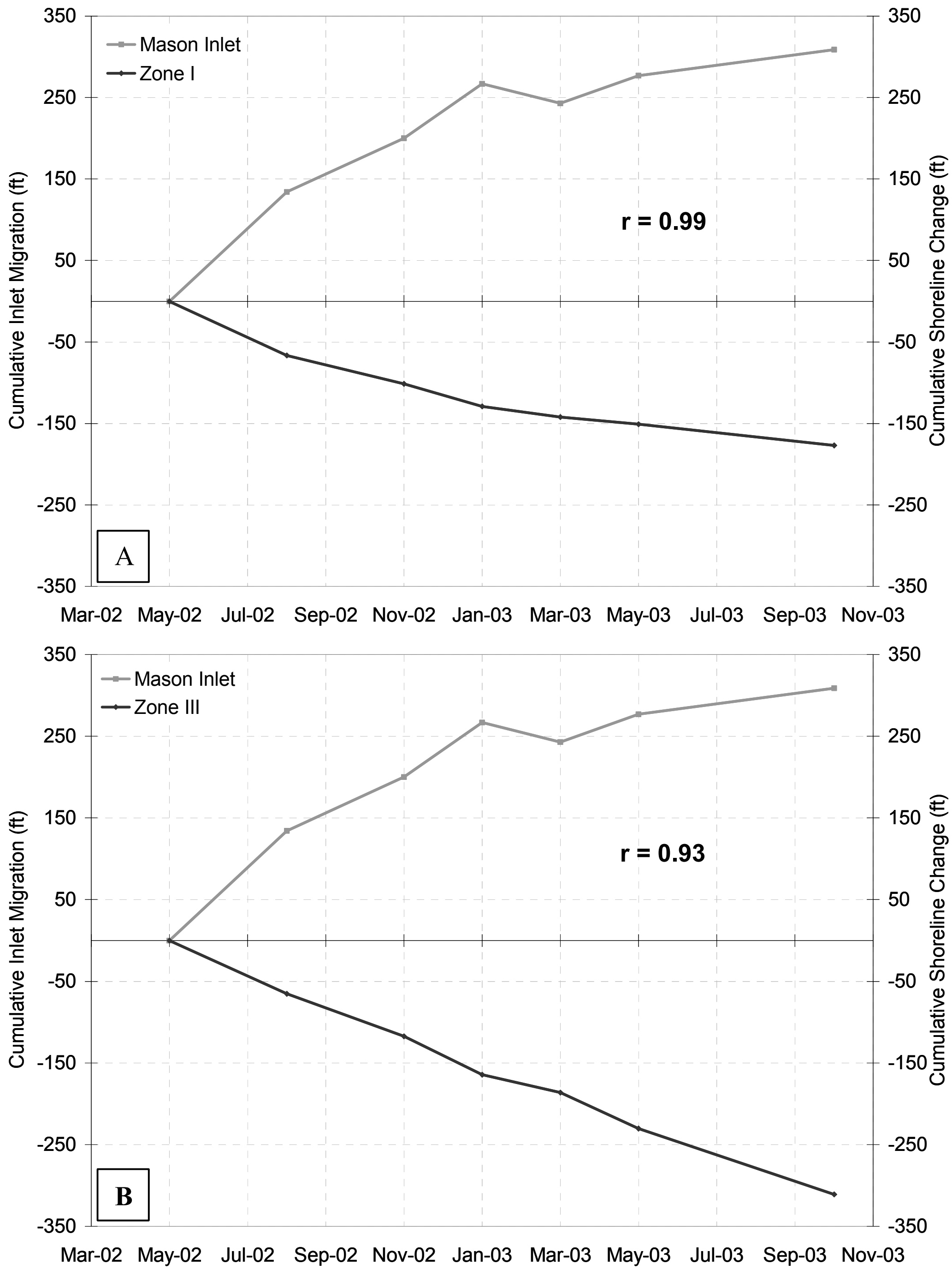

Figure 14. Graphs depicting cumulative erosion along opposing shorelines with inlet migration: (a) Wrightsville Beach shoreline erosion with southwest channel migration.
(b) Figure Eight Island shoreline erosion with southwest channel migration. Note that an increase in value of cumulative inlet migration indicates southwesterly inlet migration; whereas, a decrease in cumulative shoreline change is indicative of erosion.

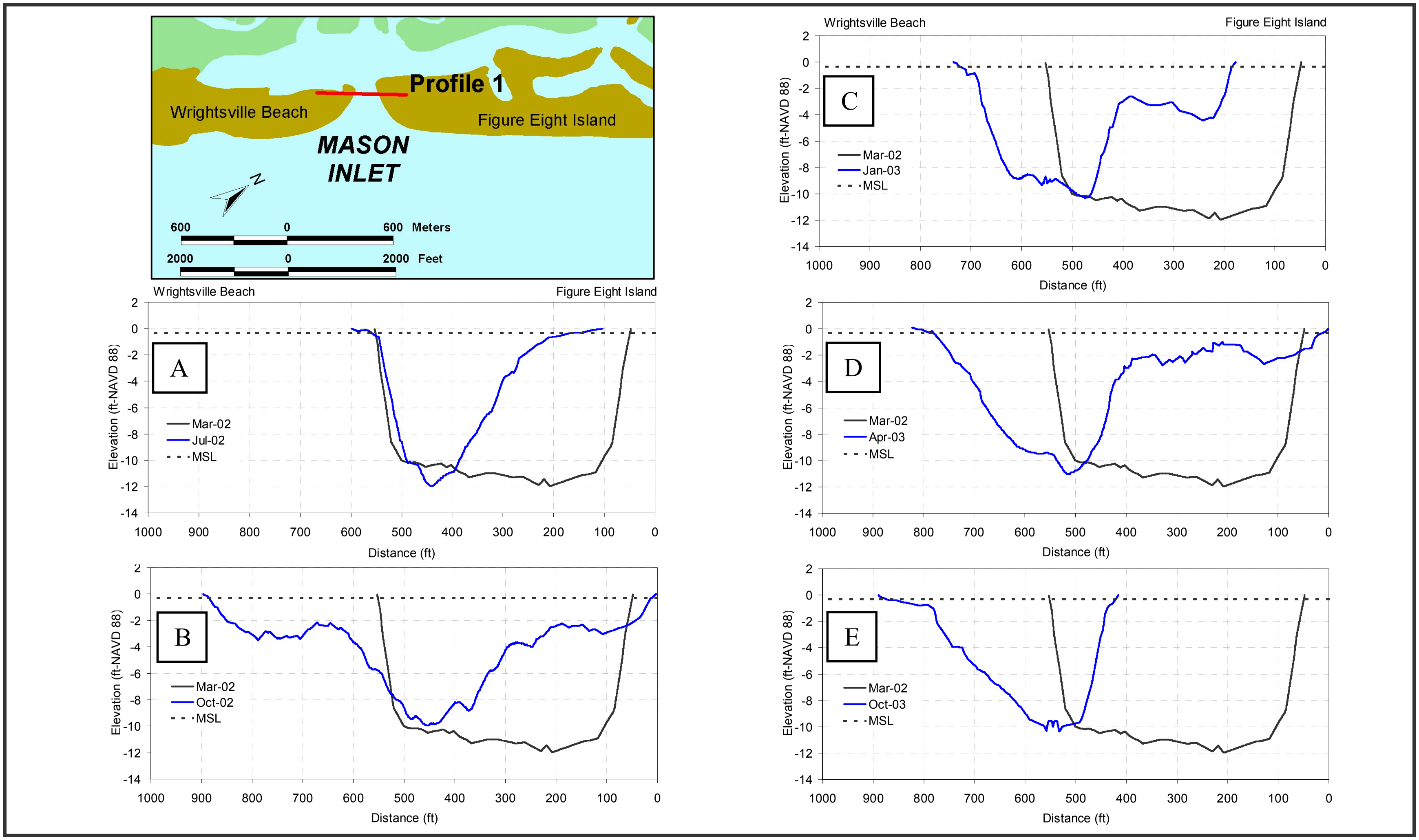

Figure 15. Cross-sections of the inlet throat taken across Profile 1. Each graph compares the March (As-built) 2002 cross-section, taken within one week following opening of the inlet, with a later cross-section.

Table 4. Throat survey data gathered across Profile 1 (see Figure 15).

Survey	Cross-Sectional Area (ft^2 under MSL)	Inlet Width (ft)	Depth (ft below MSL)	Aspect Ratio (width:depth)	Wetted Perimeter (ft)
Mar-02	4,867	502	11.6	43	505
Jul-02	2,179	414	11.6	36	416
Oct-02	3,513	873	9.6	91	875
Jan-03	2,793	539	10.0	54	541
Apr-03	3,119	768	10.7	72	770
Oct-03	2,290	453	9.5	48	454
Mean	3,127	592	10.5	57	594

decreased by 55% to 2,179 ft^2 as the channel migrated to the southwest. An increase in area of 1,334 ft^2 occurred from July to October 2002. Cross-sectional area values continued to fluctuate from 3,513 ft^2 to 2,290 ft^2 over the remainder of the study until October 2003.

Throughout the study period, dramatic changes in cross-sectional area were accompanied with changes in shape of the channel. The ebb channel's aspect ratio (width:depth) provides a good representation of variability of channel shape. A comparison of channel A_C and aspect ratio reveals a poor correlation (r = 0.18) indicating that they are not directly related. Maximum depth below MSL remained fairly constant throughout the study period fluctuating between -11.6 ft and -9.5 ft along Profile 1 (Table 4). As a result, the aspect ratio values are directly correlated to the trend in inlet width changes at MSL (r = 0.98, significant with 99% confidence). Large fluctuations in the aspect ratio were observed over the study (Table 4). Initially, a drop in value of the aspect ratio was observed, with a fairly large increase occurring between July and October 2002, with smaller shifts and a general decreasing trend of values over the remainder of the study.

Associated with these changes in shape of the channel is the adjustment of the channel's wetted perimeter. Changes in the wetted perimeter exhibited the same highly variable trend as shown by the aspect ratio and inlet width changes at MSL (Table 4). Wetted perimeter values ranged from 416 ft to as great as 875 ft throughout the study period and were all within 2 to 3 ft of the inlet width values at MSL.

Flood Shoal Transport

Tracking the flood shoal's bedform position through time revealed the overall migratory nature of the portion of shoal studied. Based on a weekly time-scale, the shoal behaved in an erratic migratory manner with a large net migration (32 ft) in the northeast direction occurring during the first week of study, minimal northerly migration of <1 ft and southerly migration of 1 ft, respectively, during the second and third weeks, and moderate shifts of 12 ft and 13 ft to the northeast over the last two weeks (Figure 16a). Net migration of the shoal for all transects revealed a strong shift to the northeast during this six-week period of concern. The mean net positional change of the shoal was determined to be 53 ft in the northeast direction, with a mean net EPR of 527 ft/yr.

Analyses performed on the shoal yielded similar results for volumetric changes between each week of the study. Calculations of volume above the -3.58 ft contour elevation estimated the initial volume of the portion of shoal of concern to be approximately 12,243 yd^3. During the first week the shoal accreted about 472 yd^3. A slight loss of 6 yd^3 was calculated for the second week, while accretion of 25 yd^3 and 57 yd^3 occurred during the third and fourth weeks, respectively. For the last week of the study a slight loss of 5 yd^3 was determined. The net volume change over the six weeks is estimated to be an accretion of approximately 543 yd^3 of material. Cut-and-fill analysis revealed a similar result for this net volume change with an estimate of 544 yd^3 of material gained (Figure 16b). Based on these data, shoaling estimates for this portion of the shoal approximated 5,345 yd^3/yr within Banks Channel.

Ebb-Tidal Delta Development

Volumetric computations were conducted for the period between March 2002 and October 2003. Based on bathymetric maps derived from field data, an ebb shoal boundary was delineated for each particular survey completed in an effort to track the development of the shoal (Figure 17). Volume and area changes determined during the analyzed period for this feature can be found in Table 5.

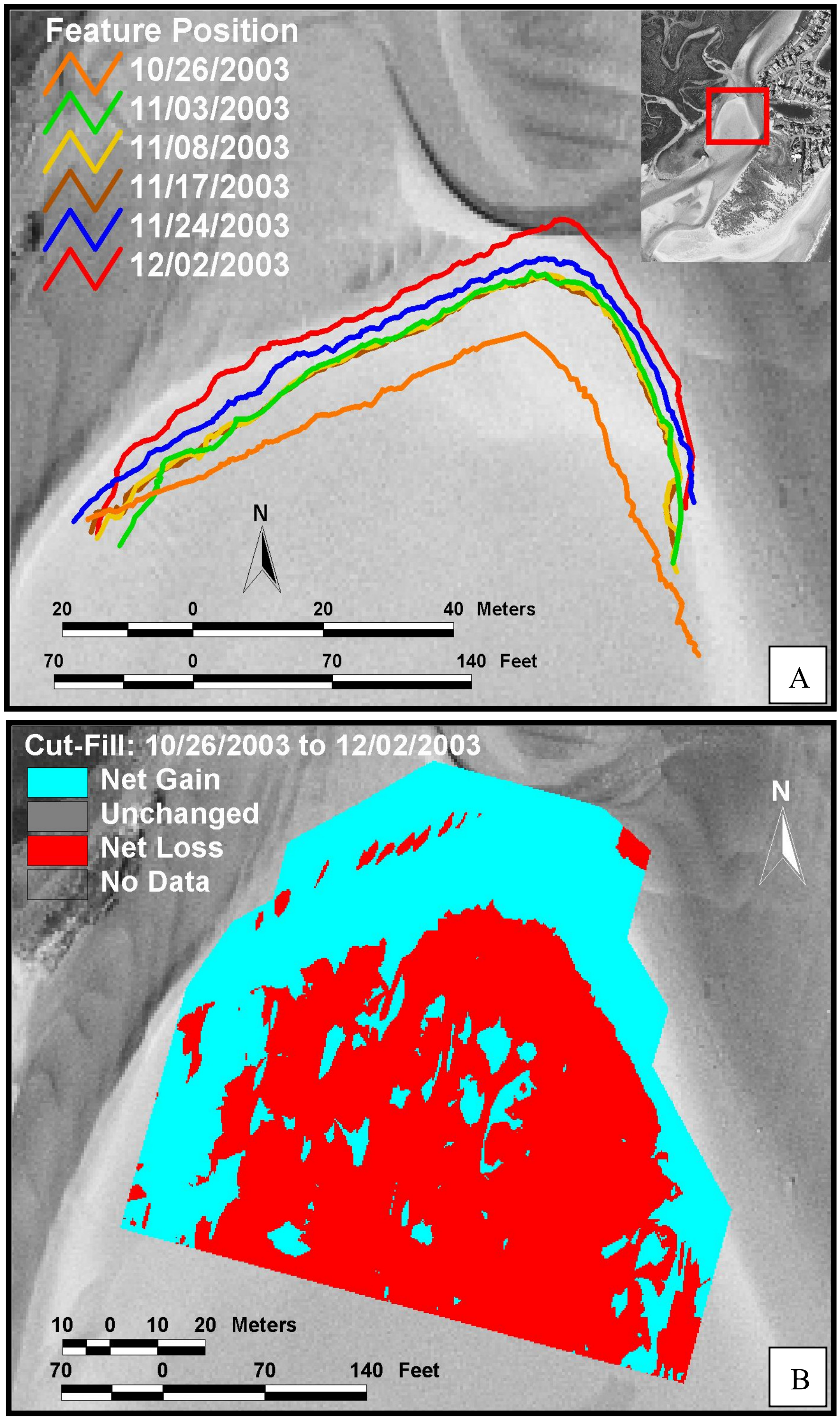

Figure 16. Flood shoal (a) feature position changes and (b) net volume change within Banks Channel.

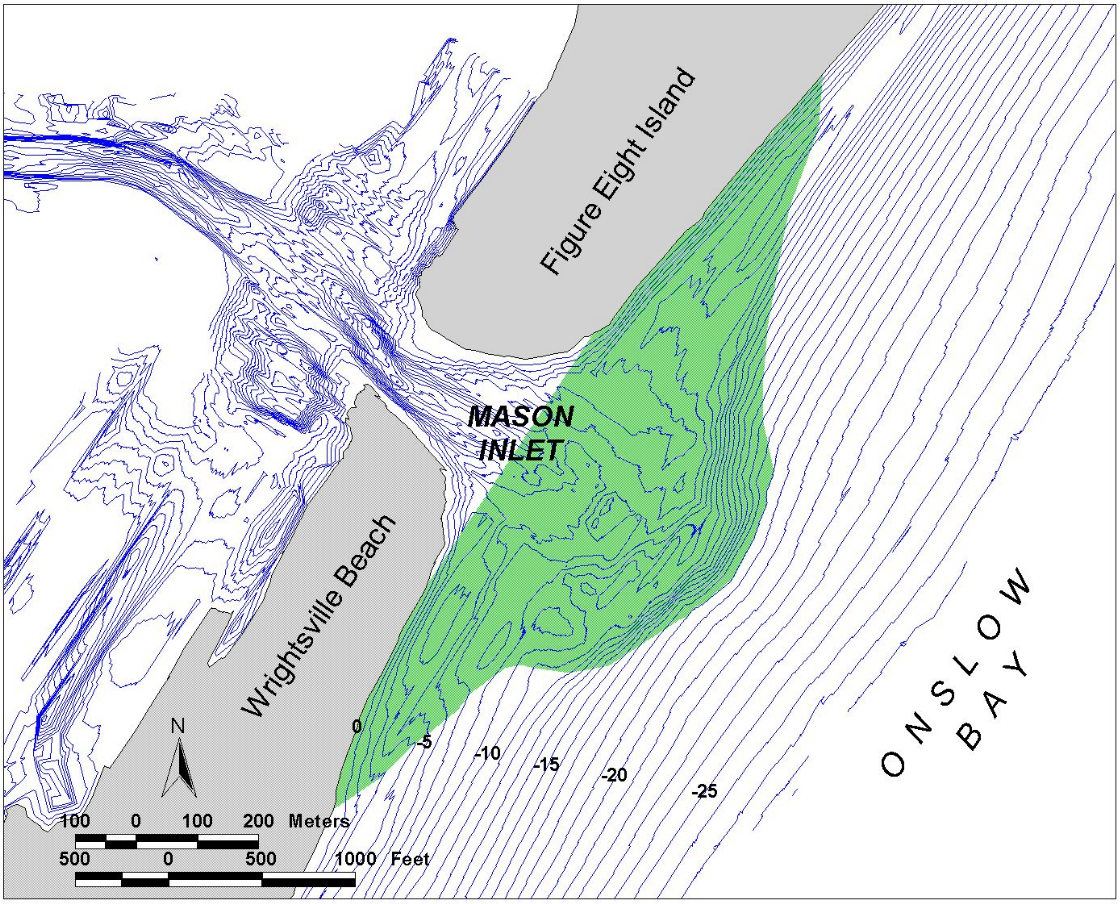

Figure 17. Post-relocation map based on July 2002 bathymetric survey depicting bathymetric map (1-ft contour interval) and delineated ebb-tidal delta area (green).

Table 5. Ebb-tidal delta development. Volumes are calculated off the March (As-built) 2002 surface and areas refer to the portion of the shoal above the March 2002 surface.

Ebb-Tidal Delta Development		
Survey	Volume (yd^3)	Planimetric Area (ft^2)
Jul-02	167,163	1,435,447
Oct-02	232,670	2,193,852
Jan-03	248,747	2,290,341
Apr-03	288,156	2,622,552
Oct-03	309,859	3,378,316
Mean	249,319	2,384,102

An accumulation of approximately 167,163 yd^3 of material encompassing an area of 1.4 x 10^6 ft^2 was calculated for the ebb shoal four months after inlet opening. Between July and October 2002 the ebb shoal area enlarged by 53% as 65,506 yd^3 of material was supplied to the shoal. ERICKSON *et al*. (2003) determined that the ebb shoal contained approximately 235,431 yd^3 by October 2002. A 1.2% difference was determined to exist between ERICKSON *et al*. (2003) ebb shoal volume (235,431 yd^3) and the October 2002 volume (232,670 yd^3) measured by the author. Growth of the shoal continued with a volume of 288,156 yd^3 and an area of 2.6 x 10^6 ft^2 measured 14 months (April 2003) post-inlet opening. Total accumulation of the ebb shoal for the 1.6 years since relocation was 309,859 yd^3 resulting in an area of 3.4 x 10^6 ft^2 by October 2003 (Table 5).

ADCP Data

Inlet Throat and Tidal Prism

All pertinent ADCP flow data pertaining to the inlet throat are presented in Table 6. Discharge measurements collected during a flood tidal flow were later manipulated for the purpose of calculating the tidal prism (T_P). Seven of the eight completed surveys within the throat were conducted during a flood tidal flow yielding a total of seven values for T_P during the course of the study. A large degree of variation between these individual T_P values exists from one survey to the next. The first ADCP survey was conducted only three weeks following the opening of the new inlet during a Spring tide with a flood range of 5.58 ft and exhibited a maximum flood velocity of 5.08 ft/s, a channel section of 4,131 ft^2, and a T_P of 259 x 10^6 ft^3. A 64% decrease in the T_P value occurred between the March 28, 2002 and July 1, 2002 surveys. The Neap flood tidal range during this survey was 3.02 ft, a reduction of 2.56 ft from the

Table 6. ADCP and tide range data for each of the eight throat surveys.

Mason Inlet Throat Parameters - ADCP Derived

Tides	Spring		Neap		Spring	Neap	Spring	Neap	Neap	Spring
Survey Date	28-Mar-2002		1-Jul-2002		25-Jul-2002	31-Jul-2002	27-Jun-2003	8-Jul-2003	5-Sep-2003	6-Oct-2003
Tidal Flow	Ebb	Flood	Flood	Ebb	Ebb	Flood	Flood	Flood	Flood	Flood
Duration (hr)	6.45	5.95	5.72	6.32	5.63	6.08	7.20	6.88	7.08	6.38
Maximum Velocity (ft/s)	4.81	5.08	2.44	3.07	4.32	3.73	2.77	3.07	3.25	3.39
Maximum Discharge (ft^3/s)	22,943.94	23,975.99	6,743.33	4,781.58	8,649.29	10,750.32	12,795.53	12,292.70	16,727.19	14,504.67
Flow Volume (10^6 ft^3)	226.21	259.28	93.89	74.01	94.50	142.27	168.01	146.53	220.63	166.30
Channel A_C (ft^2)	3,203	4,131	2,054	1,126	2,287	2,447	3,341	2,968	4,266	3,081
Inlet Minimum Width (ft)	324	336	224	172	227	237	612	545	585	439
Average Maximum Depth (ft)	13.5	14.6	15.0	10.8	14.5	16.0	13.0	12.2	12.8	13.2
*Tidal Range (ft)	5.35	5.58	3.02	2.62	3.58	3.22	3.90	4.50	4.30	4.00

*Measured by water-level meter

previous survey. Within the same month (July 1 to July 31, 2002) the T_P increased by 52% to 142×10^6 $ft^3$with the flood range increasing by 0.20 ft. The June 27, 2003 ADCP-derived T_P, an 18% increase from the previous survey almost a year earlier, was 168×10^6 ft^3. The flood range was 0.68 ft greater. Eleven days later the T_P decreased by 13%; however, the flood range increased by 0.60 ft. A relatively large T_P volume of 220×10^6 ft^3 was determined from the September 5, 2003 survey date. A large Neap flood range of 4.30 ft was measured for this survey and resulted in a 4,266 ft^2 measured channel section. The final survey occurred on October 6, 2003 with calculations yielding a volume of 166×10^6 ft^3. The mean T_P value for the entire study period was 171.0×10^6 ft^3.

Correlation between T_P and flood tidal range was calculated for the entire study period. A positive correlation ($r = 0.87$, significant at the 95% confidence level) was found to exist between these two inlet parameters (Figure 18a) and indicates that as tidal range rises or falls the T_P volume will respond in a like manner. A similar analysis conducted between the ADCP-calculated T_P and ADCP-measured A_C determined that a positive correlation ($r = 0.95$, significant at the 99% confidence level) exists (Figure 18b) between the two. This positive correlation indicates that larger A_C values result in greater T_P values or vice versa with diminished A_C values.

Feeder Channels and Flow Distribution

Concurrent with the ADCP throat surveys, monitoring of both Mason Creek and Banks Channel was conducted during select flood surveys in an effort to determine the percentage of tidal prism distributed throughout the system as the flood tidal wave propagated through the inlet. A total of six surveys within Mason Creek and four surveys within Banks Channel were conducted (Table 7). Due to the shallow nature of Banks Channel and the high degree of

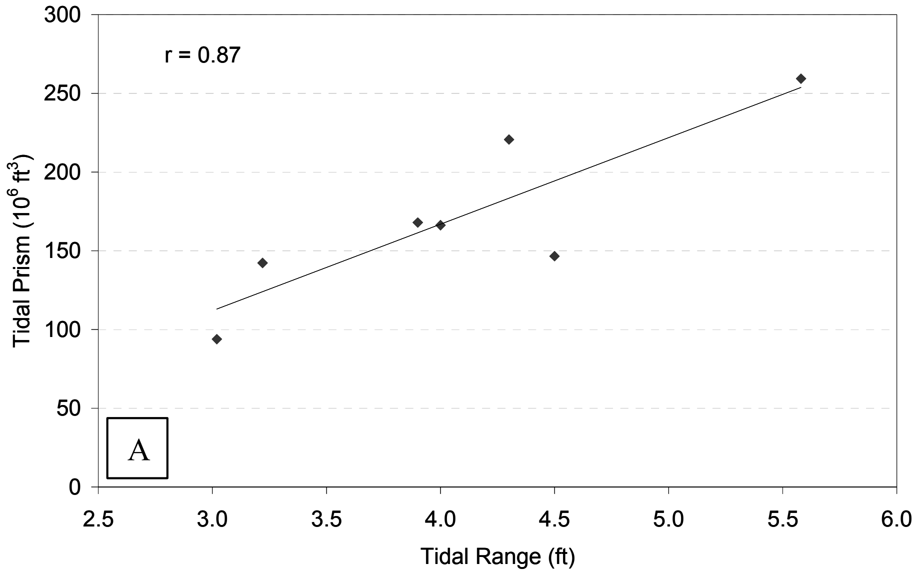

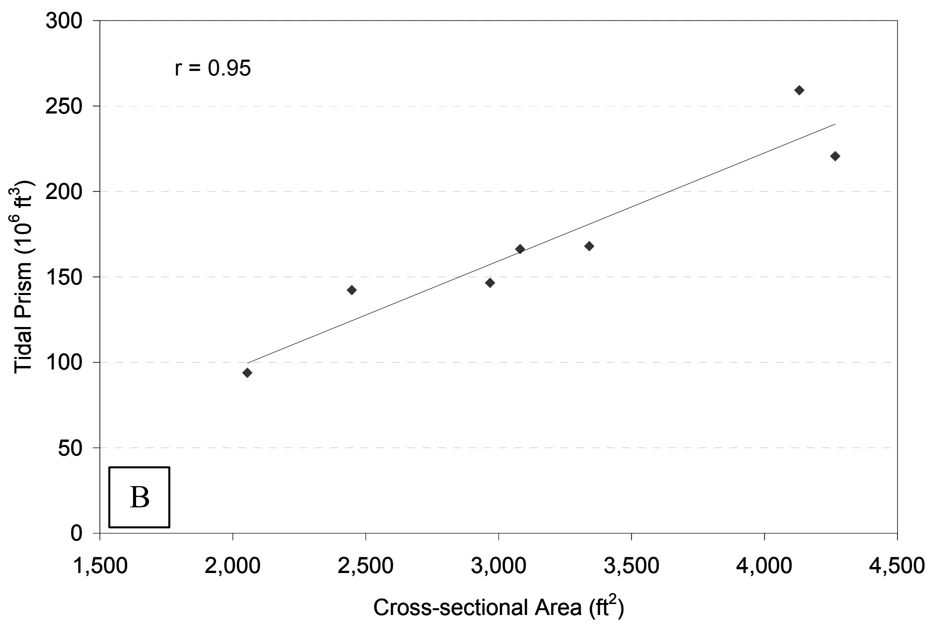

Figure 18. Inlet throat linear regression graphs indicating correlation (Pearson-r) between (a) ADCP-calculated tidal prism and tidal range and (b) ADCP-calculated tidal prism and ADCP-measured cross-sectional area.

Table 7. ADCP and tide range data for six flood surveys completed in Mason Creek at Profile 3 and the four flood surveys completed in Banks Channel at Profile 2 (see Figure 2).

Mason Creek Parameters - ADCP Derived

Survey	Flow Volume (10^6 ft^3)	A_C (ft^2)	Flood Flow (%)	Maximum Discharge (ft^3/s)	Maximum Velocity (ft/s)	*Tidal Range (ft)	Maximum Depth (ft)
1-Jul-2002	51.83	1,816	55	3,403.07	1.61	3.1	10.7
31-Jul-2002	69.58	2,089	49	4,486.08	2.16	3.2	11.2
27-Jun-2003	83.63	2,033	50	5,709.94	2.55	3.9	14.1
8-Jul-2003	73.25	1,945	50	5,884.52	2.85	4.5	14.2
5-Sep-2003	92.50	1,854	44	6,736.75	3.55	4.3	14.6
6-Oct-2003	75.85	1,740	46	5,318.36	3.02	4.0	14.3
Mean	74.44	1,913	49	5,256.45	2.62	3.8	13.2

Banks Channel Parameters - ADCP Derived

Survey	Flow Volume (10^6 ft^3)	A_C (ft^2)	Flood Flow (%)	Maximum Discharge (ft^3/s)	Maximum Velocity (ft/s)	*Tidal Range (ft)	Maximum Depth (ft)
27-Jun-2003	66.14	945	39	5,735.76	2.31	3.9	8.7
8-Jul-2003	55.95	928	38	6,346.67	2.58	4.5	8.5
5-Sep-2003	70.81	1,190	34	6,752.76	2.13	4.3	9.3
6-Oct-2003	63.93	1,297	38	6,826.01	2.26	4.0	8.7
Mean	64.21	1,090	37	6,415.30	2.32	4.2	8.8

*Measured by water-level meter

morphologic variability within this channel during the initial year following the inlet's opening, measurement of flow was impossible with the ADCP. Flow data collection within Banks Channel proved to be extremely challenging. By June 2003, a portion of the channel could be directly measured with the ADCP; however, a large flood shoal had developed within the mouth of the channel (Figure 8). This portion of the channel was submerged only during the final portion of a flood tide when the water levels were the highest. During those portions of the flood tide, WinRiver™ extrapolated the discharge across this shallow (~ 1–2 ft depth under mean high water) platform. Surveys within Mason Creek were initiated four months following the opening. The two initial surveys, conducted in July 2002, determined that 55% and 49% of the flood flow volume (T_P) entering the inlet was conveyed through Mason Creek. Surveys continued the following summer, beginning in June 2003, and estimates of flow through Mason Creek, the primary feeder channel (see Figure 3), and Banks Channel were determined to be 50% and 39%, respectively. Similar results were observed eleven days later with 50% (Mason Creek) and 38% (Banks Channel) of the flow passing through each feeder channel. This trend persisted throughout the study period with Mason Creek serving as the major conduit by which flow was distributed. Supporting evidence of the trend was evident in the last two surveys that showed 10% and 8% more flow passing through Mason Creek than Banks Channel. Overall, the mean percentage of flood flow conveyed through the separate feeder channels was determined to be 49% for the primary access channel of Mason Creek, 37% for Banks Channel, and 14% lost to the remainder of the system.

Theoretical Relationships and Comparisons

Tidal Prism and Cross-Sectional Area

The widely recognized relationship between tidal prism and inlet throat cross-sectional area was initially discovered by LECONTE (1905) and later refined by O'BRIEN (1931, 1969) who exposed the relationship's potential. JARRETT (1976) furthered understanding of the relationship by grouping inlets into separate classes based on wave energy setting and on the presence or absence of jetties. Segregating the inlets allowed Jarrett to formulate unique linear regression equations for each class. BYRNE *et al*. (1980) determined that relatively small tidal inlets situated within protected coastlines fail to apply to the predicted relationship of JARRETT (1976). Although Mason Inlet is not within a protected coastline, it is a relatively small inlet and consideration of that fact should be noted when utilizing this relationship. Utilizing the throat cross-section and tidal prism derived values from data collected with the ADCP and topo-bathymetric surveys, it is possible to make comparisons between the new inlet channel and the predicted equilibrium cross-sections derived from these regression equations. For the purposes of this study, the frequently used regression equation derived by JARRETT (1976) for the Atlantic Coast was used in order to compare the values for the mean measured tidal prism and the calculated tidal prism (Equation 1):

$$A_C = 7.75 \times 10^{-6}\, T_P^{1.05} \qquad (1)$$

where: A_C = throat cross-sectional area (ft^2) and T_P = tidal prism (ft^3). The cross-sectional area values used in Jarrett's equation represent the mean of the cross-sectional area values (A_C = 3,184 ft^2) measured during each of the seven throat surveys conducted during flood tide conditions with the ADCP and the mean of the values ($A_C = 3{,}127$ ft^2) measured across the six generated TIN surfaces. Based on Equation 1 and the A_C measured by the ADCP, the resulting calculated tidal prism was 159.8 x 10^6 ft^3. The difference between this predicted T_P (159.8 x 10^6 ft^3) and the mean ADCP-calculated T_P (171.0 x 10^6 ft^3) was approximately 7%. The resulting predicted tidal prism, based on Equation 1 and the TIN-measured A_C, was 157.0 x 10^6 ft^3; an 8% difference from the mean ADCP-calculated T_P (171.0 x 10^6 ft^3). A t-test ($t = 1.41$) determined that the difference between the mean predicted values and the mean ADCP- calculated values were not significant (p-value = 0.21). The relatively small difference (7% and 8%) and statistical insignificance between these predicted T_P values and the mean ADCP-calculated T_P values suggest that Equation 1 was a comparable method and fairly useful tool for estimating T_P (Figure 19).

Utilizing the A_C values measured during specific ADCP throat surveys and Equation 1, tidal prism values were generated that ranged from 105.3 x 10^6 ft^3 to 211.1 x 10^6 ft^3. The extreme differences between these predicted T_P values, using Equation 1 and the calculated T_P values ranged from <1% to 21%. It should be noted that the greatest difference of 21% occurred during the March 28, 2002 survey when the channel cross-section still maintained an artificial shape considered far from equilibrium. The next greatest difference, among these individual surveys, was 13% and occurred in July 2002. Over time the difference between the calculated and predicted values decreased as the channel section evolved. The individual ADCP-calculated T_P values were regressed against the corresponding predicted T_P values, based on Equation 1 and A_C measured by the ADCP. A positive correlation was determined to exist ($r = 0.97$, significant with 99% of confidence). This relationship was indicative of the comparativeness of these two

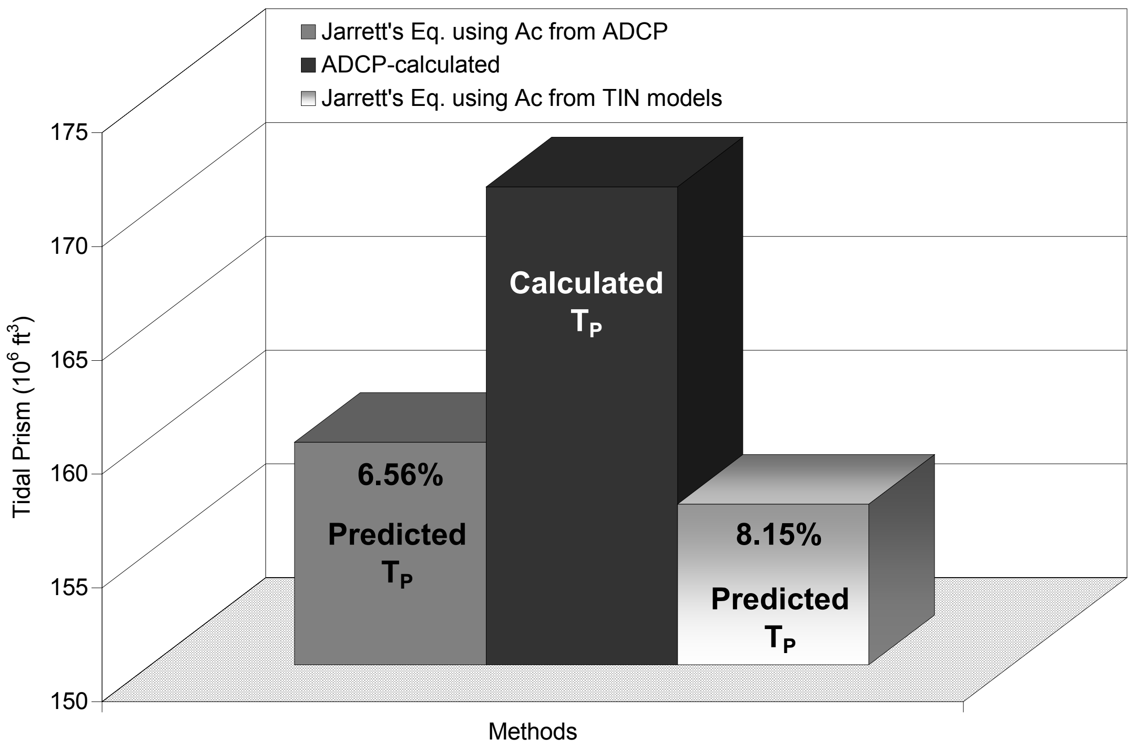

Figure 19. Bar graph illustrating differences in derived tidal prism values.

different methodologies for estimating tidal prism (Figure 20a). These two different methods were useful for T_P estimation and appeared to compare more closely as the channel evolved over the study period.

Similarly, an analysis of regression between the individual ADCP-measured A_C values and the predicted A_C values, based on Equation 1 and ADCP-derived T_P values, indicated a strong correlation ($r = 0.97$, significant with 99% of confidence) (Figure 20b). As expected, after noting the diminishing differences between the ADCP-calculated T_P and the predicted T_P, a similar trend occurred between the ADCP-measured A_C and the predicted A_C. Utilizing the T_P values calculated from specific ADCP throat surveys and Equation 1, A_C values were generated that ranged from 1,822 ft^2 to 5,294 ft^2. The differences between these predicted A_C values, using Equation 1, and the measured A_C values ranged from <1% to 28%, with the largest difference occurring on the March 28, 2002 survey. The next highest difference, when focusing on these individual surveys, was in July 2002 at 15%. As the study progressed and the inlet channel section evolved differences between these values diminished.

Ebb-Tidal Delta Volume and Tidal Prism

Previous work by WALTON and ADAMS (1976) revealed a strong correlation, by way of linear regression analyses, between the volume of sand stored in the ebb-tidal delta of an inlet and its tidal prism. According to their coastal energy classification scheme the inlets along the east coast of the U.S. (except in South Carolina), and Panhandle of Florida (Gulf Coast) fall within the moderately exposed coast range. Tidal prism measurements used in their study were based on measurements from current data obtained at the throat of an inlet or by the “cubature method”. The inlets analyzed in their study were considered equilibrated with respect to their surroundings. In order to compare the volume of material estimated to be retained in the ebb-

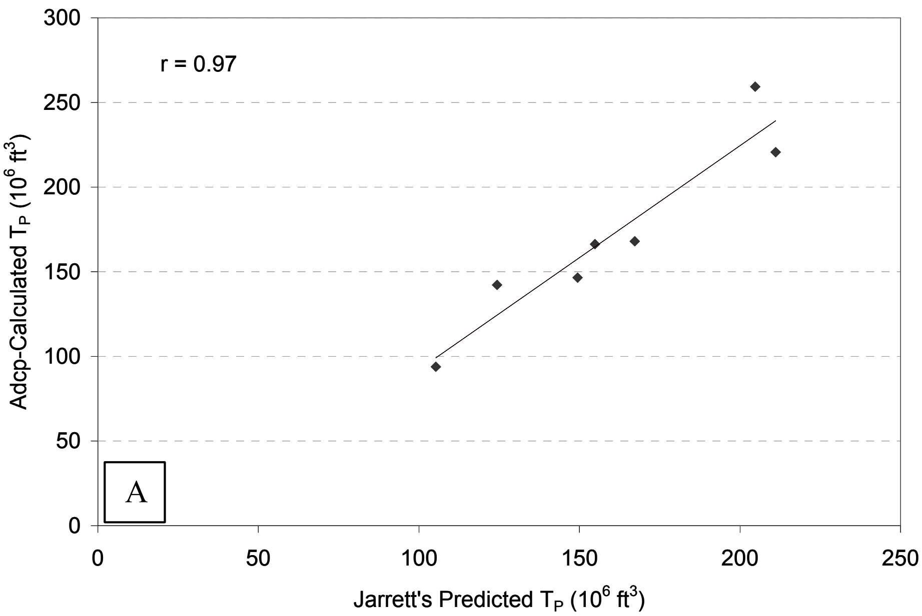

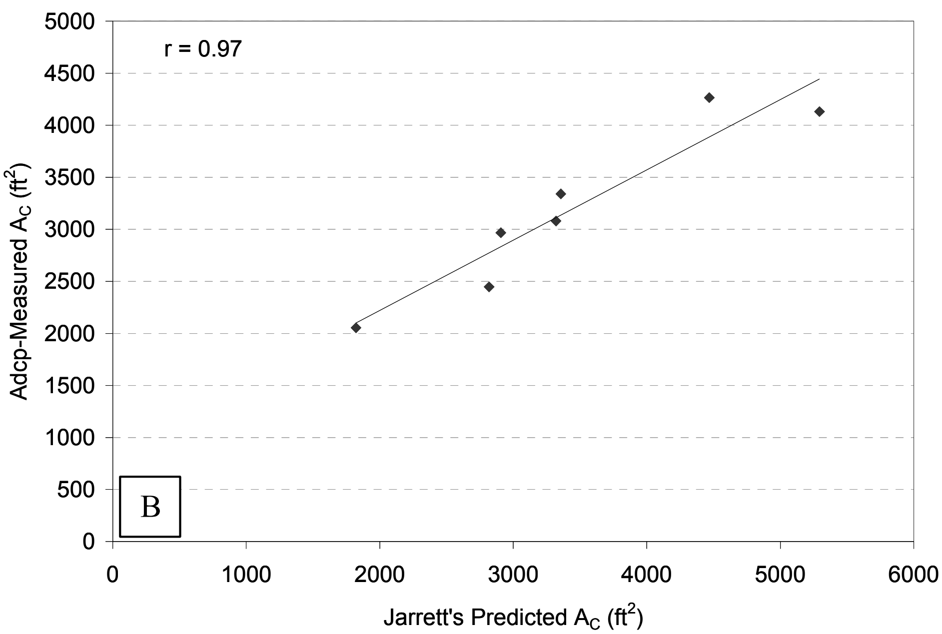

Figure 20. Linear regression graphs indicating correlation (Pearson-r) between (a) ADCP-calculated tidal prism and Jarrett's predicted T_P and (b) ADCP-measured cross-sectional area and Jarrett's predicted A_C.

tidal delta from TIN surfaces with the predictions of their empirical model, the mean ADCP-calculated Tp value was used in conjunction with WALTON and ADAMS' (1976) theoretical equation for moderately exposed coasts (Equation 2):

$$V_{ETD} = 10.5 \times 10^{-5}\, T_P^{1.23} \qquad (2)$$

where: V_{ETD} = ebb-tidal delta volume (yd^3) and T_P = tidal prism (ft^3). The T_P value used in Equation 2 represents the mean of the T_P values ($T_P = 156.3 \times 10^6\ ft^3$) calculated during each of the six throat surveys between July 2002 and October 2003. The March 2002 T_P value was not used in this analysis due to the artificial shape of the channel and the lack of an ebb shoal located offshore at that time. Based on Equation 2 and the mean T_P calculated with the aid of the ADCP, the resulting predicted ebb shoal volume was $1.26 \times 10^6\ yd^3$. The difference between this mean predicted V_{ETD} ($1.26 \times 10^6\ yd^3$) and the final directly measured V_{ETD} (309,859 yd^3) in October 2003 was approximately 75%. The final (October 2003) V_{ETD}, twenty months post-inlet opening, measured 309,859 yd^3 and comprised only 25% of the predicted volume (Figure 21).

Ebb-Tidal Delta Volume and Cross-Sectional Area

As inlet throat cross-sectional area exhibits a direct correlation with tidal prism and is considered an easier inlet parameter to measure than tidal prism, WALTON and ADAMS (1976) derived a correlation between the volume of the ebb-tidal delta and the cross-sectional area of the channel. In order to compare the volume of material estimated in the ebb-tidal delta from TIN surfaces with the predictions of their empirical model, the mean TIN-measured A_C value was

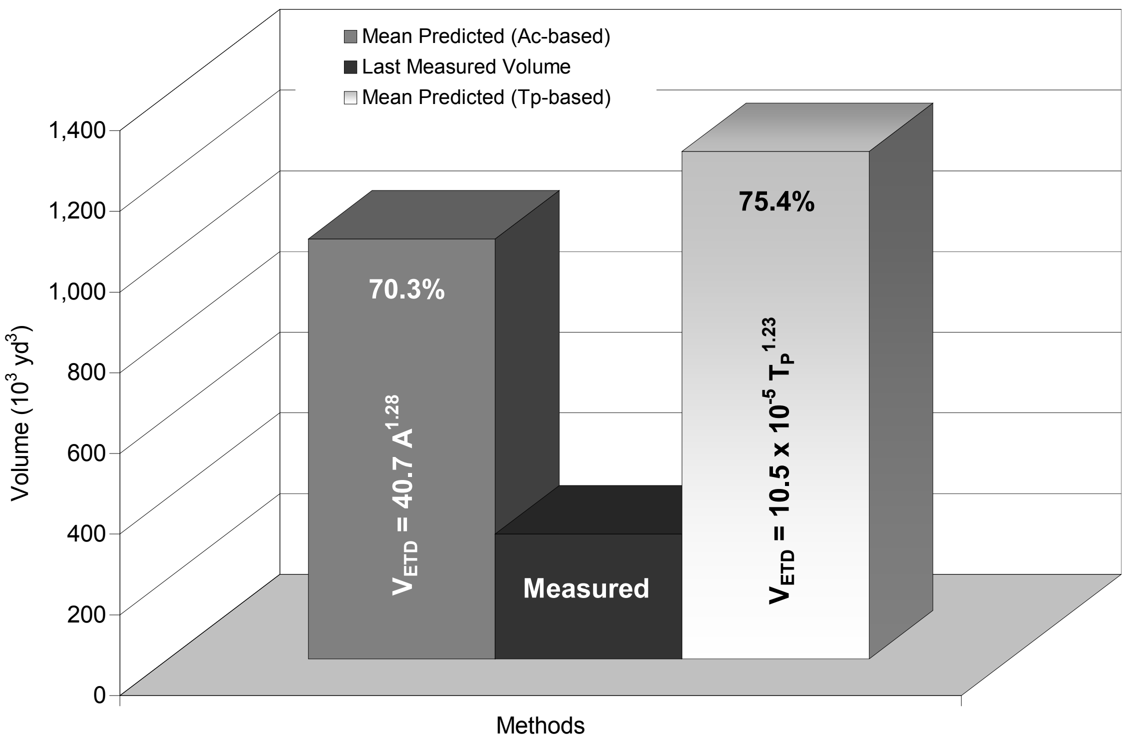

Figure 21. Bar graph illustrating differences in derived ebb-tidal delta values.

used in conjunction with WALTON and ADAMS' (1976) theoretical equation for moderately exposed coasts (Equation 3):

$$V_{ETD} = 40.7\, A_C^{1.28} \qquad (3)$$

where: V_{ETD} = ebb-tidal delta volume (yd^3) and A_C = cross-sectional area (ft^2). The A_C value used in Equation 3 represents the mean of the A_C values (A_C = 2,779 ft^2) measured across the five generated TIN surfaces between July 2002 and October 2003. The March 2002 A_C value was not used in this analysis due to the artificial shape of the channel and the lack of an ebb shoal located offshore at that time. Based on Equation 3 and the mean A_C measured across the TIN surfaces, the resulting predicted ebb shoal volume was 1.04×10^6 yd^3. Comparisons of the individual measured V_{ETD} values with this predicted V_{ETD} (1.04×10^6 yd^3) revealed that the initial July 2002 V_{ETD} (167,163 yd^3) comprised only 16% of the predicted volume. By the end of the study, the shoal increased in size with an (October 2003) V_{ETD} measuring 309,859 yd^3 and comprising only 30% of the predicted volume.

DISCUSSION

The study of Mason Inlet and its associated relocation provided a unique opportunity to not only discover what impacts an engineering effort of this magnitude imposes on an area but provided comparisons between measurements collected in the newly evolving system to predictions of what was expected to occur. The predictive regression equations of JARRETT (1976) and WALTON and ADAMS (1976) have been used in this study to predict parameters for inlet conditions that the authors may not have initially intended for use by their equations. The applicability of these equations to the newly developing system are assessed and provide a "measuring stick" of where the inlet and the parts that comprise it rank with regard to stability/equilibrium. These relationships granted insight into the performance of inlet and allowed for the comparison to other relocation efforts of a similar manner.

FREEMAN (2001) noted Mason Inlet's propensity toward infilling of its lagoon, specifically Mason Creek, with sediment since October 1971. Complete closure of the creek was becoming imminent by 1997. Infilling of the lagoon, including Mason Creek, suggested that the tidal prism had most certainly decreased over this period. Evidence of infilling and processes causing landward transport of sediment were provided in FREEMAN's (2001) study of Mason Inlet. Morphologic data, since 1997, have shown that (sandbag emplacement next to Shell Island Resort) infilling of the feeder channels continued until dredging, as part of the relocation effort, in 2002 extracted a large volume of sediment from the system. ATM (2000) estimated sand deposition within the feeder channels occurred at a rate of 75,861 yd^3/yr between 1996 and 1999. Image analysis revealed shoaling within the inlet throat along with Banks Channel and suggested constriction of flow and increased hydraulic inefficiency occurred throughout the system (Figure 7). Measurements relating to the ebb-tidal delta revealed a 17% reduction in area between 1998 and 2002. CLEARY and FITZGERALD (2003) documented a 46% reduction in cross-sectional area at the inlet throat between 1998 and 2001. Based on these findings it is safe to assume that the tidal prism continued to diminish until relocation.

Reduction in tidal prism and the flushing capability of an inlet allows wave-driven transport (littoral drift) to dominate over tidal flow (JOHNSON, 1919). As a result, littoral drift assumes the dominant role in determining the inlet's stability. Between 1974 and 1996, the inlet channel migrated southwest approximately 3,609 ft, at an average rate of 164 ft/yr (CLEARY and MARDEN, 1999). After emplacement of sandbags along the southern channel bank in 1997, the inlet channel's net EPR slowed to 29 ft/yr between 1998 and February 2002.

Stabilization of the inlet allowed the ebb-tidal delta to remain localized. As tidal prism reduction occurred the ebb-tidal delta area diminished (17% between 1998 and 2002) in response. Net accretion measured along the downdrift shoreline over this period is most likely a direct result of sediment being bypassed from the ebb-tidal delta to this section of coastline. Coupled with this was the alignment of the main ebb channel. JACKSON (2004) noted that the orientation of Mason Inlet's ebb channel switched from 133° to 111° between February 1998 and February 2002. This southeast orientation of the ebb channel resulted in a favorable ebb-tidal delta morphology that was responsible for shielding the downdrift beach from direct wave energy from the northeast while allowing sediment bypassing to occur and nourish the downdrift shoreline. Migrating swash bars welded to the downdrift shoreline forming a "shoreline bump" (Figure 10) as a result of bypassing and reversal in alongshore transport direction from wave refraction around the shoal's outer margin (see FITZGERALD *et al*., 1976). The small amount of accretion along the updrift shoreline can be attributed to several artificial nourishment efforts on the beach that occurred during 1998 and 1999 (JACKSON, 2004).

Morphologic features such as sand-clogged channels, extensive flood-tidal delta deposits, and the lack of a well-developed ebb-tidal delta are indicative of flood dominance at an inlet (LINCOLN and FITZGERALD, 1988). Features such as these are all found at Mason Inlet (Figure 7). FREEMAN (2001) concluded that flood-tidal dominance, waves, and storm-driven flow were the forcing mechanisms transporting sediment landward at Mason Inlet. Combining these physical processes with the inlet's morphologic changes plays an integral role in reducing the tidal prism and maintaining a southwesterly migration trend.

Based on image analysis pertaining to the post-relocated inlet system (1.6 years following relocation), lagoonal infilling is quite evident as Mason Creek, Banks Channel, and the sedimentation basin have all infilled with varying amounts of sediment (Figure 8). Early in the formation of the new inlet, movement of the ebb channel initiated. Post-relocation migration rates initially were quite elevated during what is believed to be an adjustment period experienced by the new inlet. Artificial placement and excavation of the ebb channel across the southern spit of Figure Eight Island where no offshore shoals existed resulted in a scenario where the channel was afforded little protection from wave energy and tidal influence. That forced the inlet to react in a swift manner whereby it sought to adjust rapidly to its surroundings. Migration reflects only a small part of the overall adjustment the inlet underwent during the initial months following the opening of the channel. Net EPR (migration rate) incrementally diminished with time after the peak migration rate was attained only five months after opening. Lowering of the net EPR is indicative of the inlet exiting its initial adjustment period and entering into some degree of balance with the surrounding forcing parameters (Table 3).

Inlet migration continues to influence shoreline change along the neighboring barrier islands. Net erosion dominated along the updrift and downdrift shorelines after relocation (Figure 9). Post-relocation, cumulative erosion along the neighboring shorelines of Figure Eight Island and Wrightsville Beach has been linked to the inlet's southwest migration. High correlation coefficients between these parameters for both Figure Eight (0.93) and Wrightsville Beach (0.99) support this notion (Figure 14). Closure of the original inlet resulted in the ultimate collapse of the ebb-tidal delta (Figure 2g). As tidal flushing was reduced, wave energy processes dominated and the ebb shoal was pushed up against the nearshore zone providing natural nourishment to this section of shoreline between Transects 11-13 (Figure 6). The pre-relocation "shoreline bump" (Figure 10), seaward of the resort complex between Transects 4–10, eroded as the shoreline sought to assume a more uniform orientation in alignment with the new inlet conditions. Similarly, the erosion stretching updrift from the new inlet can be attributed to the formation and adjustment of the new inlet and its ebb-tidal delta. It should be noted that the post-relocation updrift shoreline was nourished (Figure 2b and 2c) during the relocation's construction phase (February 2002). Post-relocation analysis of shoreline position effectively began with the May 2002 photographic set, three months following the nourishment and tracked the performance of the nourished shoreline. It is expected that a large amount of material that eroded from the recently nourished updrift beach was transported into the inlet and deposited as flood shoals or incorporated into the formation of the new ebb-tidal delta. Previous work (OERTEL, 1977; FITZGERALD *et al*., 1978; FITZGERALD, 1996) has determined that increases in the volume of the ebb shoal relate to erosion of neighboring shorelines. It is believed that inlet migration coupled with formation of the new ebb shoal and post-construction sorting of beachfill is responsible for the erosion trend observed along the updrift segment. Along the downdrift reach, collapse of the original offshore shoal combined with the new position of the inlet, in a more northerly position, has translated the shoreline to a more landward position (Figure 9).

Morphologic features and trends occurring post-relocation that mimic those that occurred prior to relocation at Mason Inlet include sand-clogged channels, extensive flood-tidal delta deposits, eroding shorelines, and migration. Flood tidal dominance appears to remain true for this system. Water-level data collected within the lagoon portion of the inlet system provides partial input into why this area still accumulates sand.

HAYES (1975) suggested that, of all process variables, variations in tidal range influence the greatest degree of large-scale changes in the morphology of sand accumulation. Based on the classification scheme devised by HAYES (1979) and the measured mean tidal range of 3.28 ft, Mason Inlet falls within the extreme upper limit of the microtidal category. Comparisons of flow durations between the flood and ebb one-quarter tidal cycles, at least within the backbarrier portion of the inlet system, revealed a consistent trend of longer ebb durations than flood by 1.17 hrs, 1.20 hrs, and 0.75 hrs under Spring, Neap, and normal conditions, respectively (Table 2). Although tidal dominance cannot be definitively stated based solely on these data alone, the shorter flood durations suggest that this post-relocation system was exposed to some degree of flood bias. The neighboring inlet system to the north exhibits a similar tidal duration trend. KNIERIM (2003) determined that longer ebb (6.78 hrs) than flood (5.63 hrs) durations occur at Rich Inlet. Tidal duration asymmetry (flood greater than or less than ebb) within an inlet causes the dominance of either flood or ebb-tidal currents and subsequently dictates the direction of net sediment transport through an inlet (BOONE III and BYRNE, 1981; ZARILLO, 1986). FITZGERALD (1988) suggested that flood duration asymmetry explains the dominance of flood tidal currents at the throat of an inlet.

Inlet flood dominance is further supported by flood and ebb flow data derived from initial ADCP surveys at the inlet throat. Preliminary ADCP surveys (March 28, 2002 and July 1, 2002) measured flow during consecutive flood and ebb tides (Table 6). Throat survey (ADCP) data showed that the mean flood duration (5.84 hrs) was 0.55 hours shorter than the mean ebb duration (6.39 hrs) for these two surveys. Shorter flood durations indicate greater flood flow velocities when assuming that the flood and ebb flow volumes are nearly equal. However, flow volumes were found to be unequal, most likely due to tidal range inequality. Flood flow volumes exceeded ebb volumes by 33.07 x 10^6 ft^3 and 19.88 x 10^6 ft^3. Maximum average flood discharge was also found to be greater than its ebb counterpart by 1,032.05 ft^3/s and 1,961.75 ft^3/s. These findings indicate that this inlet was influenced by a time-velocity asymmetry in which flood flow is predominantly shorter and of a greater average velocity/discharge than the ebb flow.

Flood flow volume inequalities have been documented in several other tidal inlet hydrographic investigations (MILITELLO and KRAUS, 2001; Waterway Surveys and Engineering *et al*., 2001; KNIERIM, 2003). Differences in flood and ebb tide amplitudes along with out-of-phase water levels with tidal currents are related to these inequalities. Determining the reason for inequality in flow volume between the flood and ebb tides can be difficult to identify for a particular inlet system. Extraneous variables such as freshwater inputs and shifting winds can play an integral part in affecting the volume of water passing through an inlet. Adding to the complexity in understanding these inequalities is the dynamic nature of circulation patterns usually found throughout an inlet system.

Previous work focusing on inlet morphology suggests that the majority of inlets situated within this region of the Georgia Bight are flood dominant (HAYES, 1994). The nearby Rich Inlet system, as described by KNIERIM (2003), demonstrates a time-velocity asymmetry with shorter flood durations and greater average flood velocities than ebb. Flood dominance documented at a large number of tidal inlets along the East coast of the U.S. has been related to interior basin characteristics (MOTA OLIVEIRA, 1970; AUBREY and SPEER, 1985; ZARILLO and MILITELLO, 1999). Inlet-lagoon systems characterized by open bays or bays filled with subaerial marsh at low tide tend to exhibit shorter flood tidal durations and flood current dominance (MOTA OLIVEIRA, 1970; AUBREY and SPEER, 1985). The backbarrier of Mason Inlet could be classified as such (Figure 8). An investigation of several well-mixed, shallow inlet-lagoon systems, similar to Mason Inlet, has revealed that tidal asymmetry greatly affects an inlet's evolution and that morphologic changes are linked to reversals in velocity dominance over time (FRIEDRICHS *et al*., 1992). Flood dominance would provide an explanation in part for why the lagoon is observed infilling with sediment. AUBREY and SPEER (1985) attributed flood dominance within Nauset Inlet, Massachusetts, to a lack of non-linear basin filling associated with channel friction related to the presence of high (supratidal) marsh.

FREEMAN (2001) suggested that processes such as flood dominance, waves and storm-driven flow were the primary mechanisms by which sediment was transported landward at Mason Inlet prior to relocation. Sedimentological data gathered by FREEMAN (2001) within the inlet system determined the sediment to be composed mainly of medium to fine grained quartz sand. The critical threshold velocity, or the minimum velocity necessary to erode and transport sand of this size in 68° F seawater and under steady flow conditions, was estimated at approximately 0.98 ft/s (MILLER *et al*., 1977; FREEMAN, 2001). For the purposes of this study, assuming the sediments comprising the ebb-tidal delta, throat, and feeder channels have remained the same post-relocation; the threshold value is assumed to be the same after relocation. ADCP data collected within the throat, Mason Creek, and Banks Channel indicate that this critical threshold value was exceeded at these locations for a majority of each tidal phase measured (Tables 6 and 7). Thus, it seems the tidal currents are of sufficient magnitude to erode and transport medium to fine grained sand within a tidal cycle. Based on the MEYER-PETER and MULLER (1948) assumption that bedload transport is a function of tidal velocity, these eroded sediments will be transported in the direction of tidal asymmetry and residual currents.

Further evidence of infilling and sedimentation within the backbarrier is corroborated with findings pertaining to the 37-day flood shoal monitoring within Banks Channel (Figure 5). Tracking of an isolated bedform feature located on the shoal revealed a mean net position change of 43 ft to the northeast (landward) over a six-week period, effectively spanning three Spring and Neap tidal phases (Figure 16a). Shoal volume within the area studied accreted a net volume of approximately 543 yd^3 of sand during this same period (Figure 16b). Analysis of water-level and flow data, collected and provided by Erickson Consulting Engineers, Inc. (ECE), pertaining to this period revealed that the mean ebb duration (6.62 hrs) exceeded the mean flood duration (5.80 hrs), the mean flood-tidal range (3.67 ft) exceeded the mean ebb-tidal range (3.65 ft), and mean maximum flood velocity (0.73 ft/s) exceeded the mean maximum ebb velocity (0.62 ft/s). These data were collected within Banks Channel (Figure 3) and are indicative of flood dominance. Offshore wave data, obtained from the National Data Buoy Center (NDBC, 2003), analysis determined that only minimal changes in significant wave height (± 0.13 ft) and period (± 1.62 sec) occurred over the five-week period.

These wide-ranging parameters, thought to be pertinent in influencing sediment transport, were explored in an effort to understand what mechanisms caused the shoal to evolve as it did. The relatively large accretion event and northeast shoal migration that occurred between the first and second surveys is difficult to explain with certainty based solely on these data alone. Normal expected shifts in the flood and ebb ranges and durations were observed during the 37-day study period and suggest that there was not an atypical tidal influence on the shoal. Similarly, wave data suggest that there was not a noteworthy weather event offshore during this period that potentially could have resulted in large waves entering the inlet and transporting large volumes of material. Flow data, collected by ECE, recorded mean maximum velocities much slower than the 0.98 ft/s critical threshold velocity necessary to erode and transport the sediment type found in this channel.

It is believed that Banks Channel flow data collected by ECE are a poor indicator of the flood currents that influenced this particular shoal complex. Reasons for this assumption are based on the ADCP data collected for this study and the location chosen by ECE for collection of current data within Banks Channel (Figures 3 and 5). A relatively large mean discrepancy of approximately 1.02 ft/s was determined to exist between the faster ADCP-measured and slower ECE-measured flood velocities. These differences in flow velocity are evident from the October 6, 2003 ADCP flood survey within Banks Channel when compared to ECE data gathered during the same tidal stage (Figure 22). The slower velocities measured by ECE are most likely related to the moored location of the instrument in a flow-protected portion of the channel behind the flood shoal, whereas the ADCP measurements were conducted closer to the inlet throat where faster velocities are expected to exist (Figure 5).

Consequently, it is believed that the shoal was not affected by an atypical climatic or tidal event. However, the shoal was most likely migrating under normal conditions and simply reached a point within the channel where further migration and shoal accumulation naturally diminish. This would explain the large initial shift and accumulation early in the study and the more subdued changes hence. Aerial photographs reveal that prior to the study the shoal of concern existed further southwest and that during the study it migrated into a narrowing section of the channel (see Figure 8). It is expected that to continue to transport large volumes of material further northeast and landward much larger tidal ranges (e.g. perigean spring tide) or a large climatic event would have to occur.

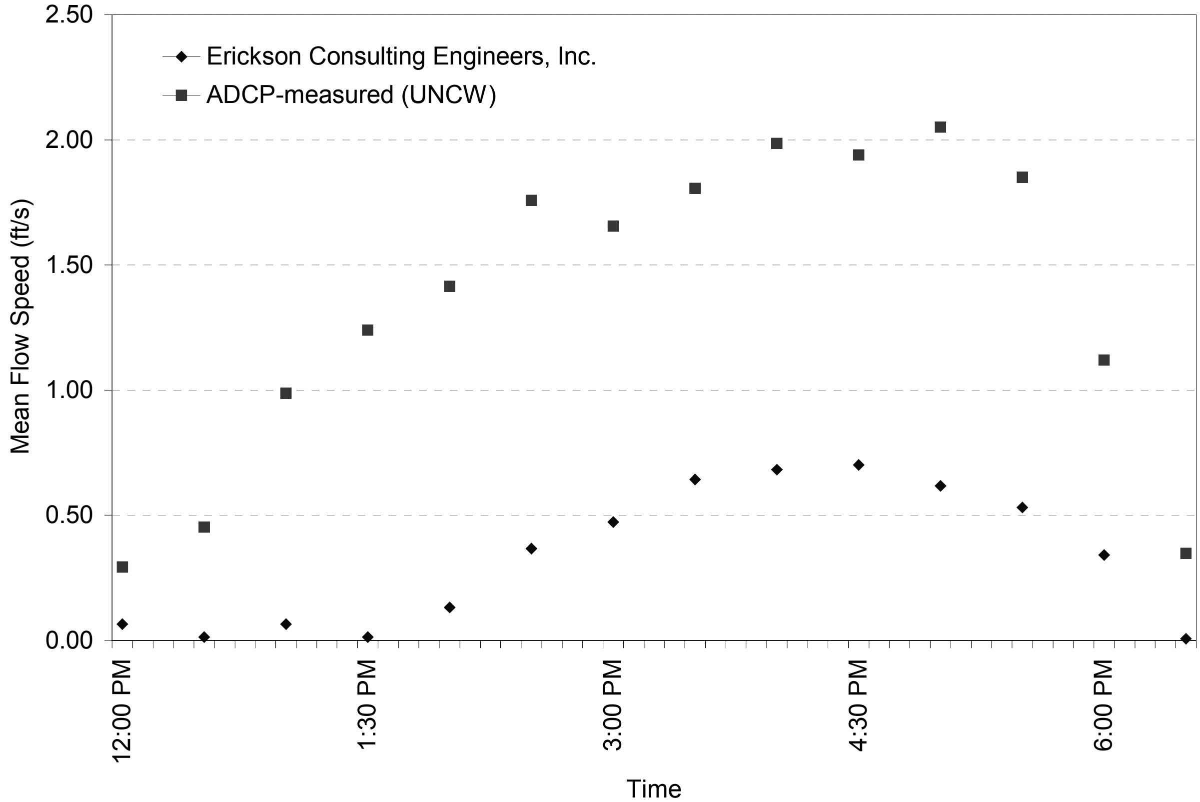

Figure 22. Flow speed comparison between data measured by the ADCP and Erickson Consulting Engineers within Banks Channel on a flood survey (10/6/2003).

Despite the fact that the T_P values varied throughout the study period, the percentage distribution of flow through the individual feeder channels remained relatively constant after the initial adjustment period (Table 7). Immediately following the inlet's opening, ERICKSON *et al*. (2003) determined, tidal flow distribution was nearly equal with 51% and 49% of the flood volume (T_P) continuing through Banks Channel and Mason Creek, respectively. Shortly thereafter, during the months of April and May 2002, predominant flow distribution gradually shifted from Banks Channel (35%) to Mason Creek (65%). This trend persisted throughout the remainder of the study with an overall mean flood flow distribution of 49% in Mason Creek, 37% in Banks Channel, and 14% lost to the remainder of the system. Compilation of these data suggest that the percentage distribution is independent of the tidal range because these surveys were conducted during tidal fluctuations differing by as much as 1.40 ft.

Reasons are varied for the characteristic flow distribution that has been observed and are suspect to be related to specific physical parameters of the feeder channels that include, channel A_C and shape, depth, and shoaling nature of the channel. Comparisons of channel characteristics between the primary feeder channels of Mason Creek and Banks Channel indicate marked differences. Mason Creek appeared to be the dominant feeder channel, with a more hydraulically efficient channel shape (semi-circular) with greater hydraulic radius and depth when compared to that of Banks Channel (Figure 23) (MANNING, 1891). Cross-sectional areas of the channels were noticeably different with Mason Creek maintaining a mean channel area 823 ft^2 greater than Banks Channel over the study period. Maximum depths within Mason Creek ranged from 10.7 to 14.6 ft and 8.5 to 9.3 ft in Banks Channel (Table 7). Shoaling was characteristically higher in Banks Channel with larger flood shoals occupying a majority of the channel's expanse (Figures 8 and 23). As determined by MANNING (1891), channels

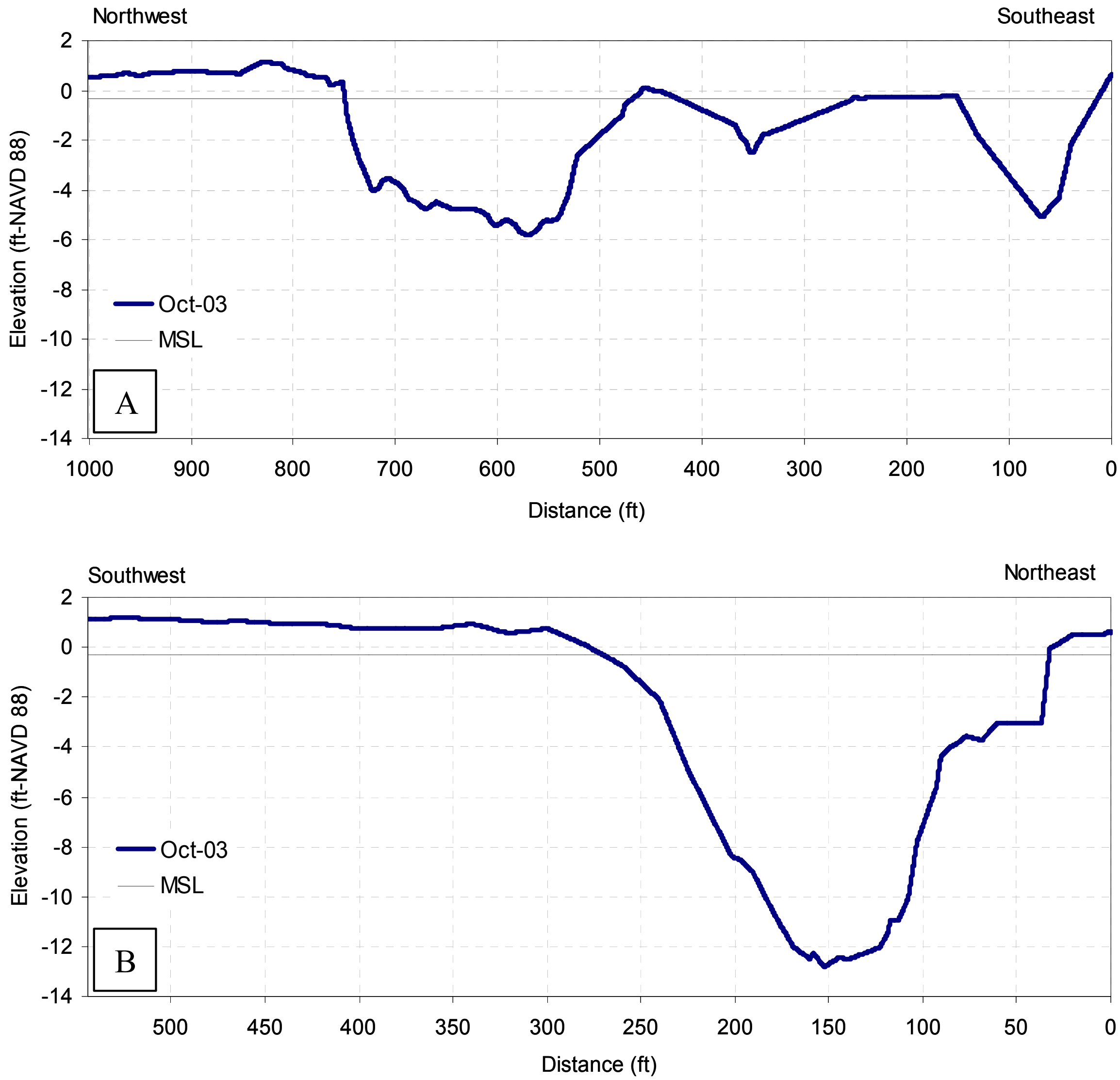

Figure 23. Feeder channel cross-sections measured during October 2003: (a) Banks Channel measured along Profile 2 and (b) Mason Creek measured along Profile 3. Note change in distance scale between (a) and (b).

characterized by uniform hydraulic radii are more prone to hydraulic efficiency. Greater cross-sectional area, depth of channel, uniform hydraulic radii, and less deposition all contribute to increasing the hydraulic efficiency of a channel by decreasing the frictional forces acting on flow.

Mason Creek's physical characteristics favor flow efficiency and thus dominates distribution of flood volume as the tidal wave propagates landward. Development of shoals within the sedimentation basin, located at the confluence of Mason Creek, Banks Channel, and the inlet channel, has also impeded flow to the north through Banks Channel (Figure 8). Upon opening of the inlet, Banks Channel was devoid of sediments; however, with the evolution of the system flood shoals formed within the lower reaches of the channel becoming emergent in select areas that narrowed and lengthened the channel. Evolution and migration of the inlet since opening has lengthened flow distance between the inlet throat and the mouths of Mason Creek and Banks Channel. As a result, the orientation of Mason Creek with respect to the throat has changed from one of direct alignment to a more circuitous route in the form of an "s"-shaped curve (Figure 8). This circuitous flow path is in part responsible for why flow percentages within Mason Creek decreased from 65% to 46% as the channel connecting the creek and throat lengthened and shoaled (Table 7).

Aspect ratio (width:depth) measured at the inlet throat may determine overall sediment transport patterns. BOON and BYRNE (1980) suggested that, with regard to a tidal inlet, the configuration of the main channel and the aspect ratio of the throat might determine flood or ebb dominance. An increase in the value of the aspect ratio suggests that a channel is tending towards hydraulic inefficiency and perhaps flood dominance assuming that the cross-sectional area of the channel remains constant. As the aspect ratio increases, within a channel of constant cross-section, the channel effectively widens and shallows. Because this assumption is based on a constant cross-section, difficulty arises in applying it to an evolving throat. Ignoring that the channel section changed, the aspect ratio indicates that this inlet initially increased in efficiency and then experienced decreased efficiency after a period of adjustment to the system (Table 4).

Perhaps over a longer period, in regard to Mason Inlet, the aspect ratio could provide an indication of how hydraulic inefficiency relates to tidal dominance. However, due to the relatively early development stage during which the inlet was studied, the wide range of width:depth values, and the constantly changing cross-section it is difficult to relate aspect ratio with tidal dominance with any certainty. Wetted perimeter values were also limited in their ability to be related to tidal dominance. These determined values were extremely variable over the course of the study due mostly to changes in cross-sectional area (Table 4). Under a constant channel area scenario, larger wetted perimeter values would be indicative of a greater area of frictional resistance to the flow of water resulting in decreased hydraulic efficiency and perhaps flood dominance.

Changes in the throat cross-section relates to another significant parameter of an inlet, the tidal prism (T_P), as determined by several previous studies (LECONTE, 1905; O'BRIEN, 1931 and 1969; NAYAK, 1971; JARRETT, 1976). A large degree of variation between the individual T_P values existed between the different surveys completed. Similarly, variations in cross-sectional area values existed as well. A high positive correlation (r = 0.95) between the ADCP-measured A_C and ADCP-calculated T_P for Mason Inlet supports that changes in the cross-section results in similar shifts of the tidal prism or vice versa (Figure 18b). It should be noted that the September 5, 2003 ADCP survey was conducted when Hurricane Fabian (Category 3) passed offshore Wrightsville Beach causing wave heights to reach 6.7 ft (NDBC, 2003). The higher than expected T_P value for this survey could be attributed to this event. Fluctuation in the tidal range of an inlet system also deserves consideration with regard to the impact on T_P. KNIERIM's (2003) study of Rich Inlet, the northern neighboring inlet, determined that tidal range shifts are directly related to variations in the T_P volumes of that system. Although an attempt to conduct surveys within Mason Inlet on days when the flood range approximated 4.00 ft, the actual range (Table 6) usually deviated from the predicted, creating a situation where the T_P was measured under varying tidal range conditions. As a result, comparison between these two parameters revealed that a high correlation exists (r = 0.87) for this inlet as well and indicates that greater ranges in the tide will be followed by larger T_P values or lower ranges followed by smaller T_P values (Figure 18a).

Error relating to ADCP-based determination of T_P is rooted in the instruments discharge measurements and the software's estimation of unmeasured subsections of the throat (Figure 4). Associated with the changes in shape and A_C of the throat a sizeable spit platform along the southern tip of Figure Eight Island developed between July 2002 and June 2003 (Figure 8). Due to the shallow nature (<2 ft at high water) of this platform direct measurement with the boat-mounted ADCP was impossible. An attempt was made to quantify the percentage of flow estimated by the ADCP when the spit platform along the Figure Eight shoulder was submerged under high water. Under worst-case conditions, approximately 15% of the T_p volume would be comprised of estimated flow over the platform during the 2003 summer surveys. RDI technical support analyzed portions of the ADCP data from these surveys and verified that the directly measured central subsection and top and bottom estimated subsections performed as expected for the conditions of this inlet. Thus, the development of the spit platform resulted in the largest obstacle to determination of T_P; however, it seems it was only a minor issue since it existed solely during the 2003 survey period and affects a small percentage (<15%) of those T_P values.

Utilization of tidal range readings to predict the T_P is not the only tool available for this system when attempting to estimate T_P. Upon consideration of JARRETT's (1976) A_C and T_P relationship, a high correlation ($r = 0.97$) between the predicted T_P, based on Equation 1 and A_C measured by the ADCP, and the individual ADCP-observed T_P values shows a relationship indicative of the comparativeness of these two different methodologies for estimating tidal prism (Figure 20a). However, tidal range fluctuations, climatological data (e.g. wind), wave conditions and freshwater inputs should all be considered, because they cannot be accounted for, when attempting to use an empirical relationship such as Equation 1. Direct field measurements (e.g. ADCP) allow the combined effects from these factors to be monitored and quantified and most likely provide a better estimate of T_P. The percentage differences (7% and 8%) between the ADCP-calculated T_P and Equation 1-derived T_P values are most likely related to extraneous factors such as wind and waves (Figure 19).

Another implication worthy of consideration is the issue of A_C equilibrium with the inlet system. JARRETT's (1976) empirical relationship was based on inlet A_C's equilibrated to their unique surrounding conditions. Obviously, this becomes an issue of concern for the current study. Unfortunately, there is no established definition for the determination of channel A_C equilibrium. KANA and MASON (1988) determined that the relocated Captain Sams Inlet achieved channel A_C equilibrium within 250 days after opening with a measured equilibrium value within 5% of the area predicted by the empirical models of O'BRIEN (1969) and JARRETT (1976). Interestingly, the predicted values of A_C for Mason Inlet began closely approximating the measured A_C values (0.5% difference) 477 days after inlet opening and continued to remain under 8% difference for the remainder of the study. Due to the high correlation (r = 0.97) between the individual ADCP-measured A_C values and the calculated A_C values (Figure 20b), based on Equation 1 and T_P measured by the ADCP, equilibration of the channel A_C was plausible, considering JARRETT's (1976) equation was based on equilibrated A_C values. Based on the findings of KANA and MASON (1988) for a relocated inlet with similar physical parameters and the calculated high correlation (r = 0.97) between the predicted and measured A_C's it seems that channel A_C for Mason Inlet may have equilibrated at a mean value of approximately 3,414 ft^2. This mean value (3,414 ft^2) is within 7% of the area predicted by the empirical relationship of JARRETT (1976).

Inspection of the throat's aspect ratio (width:depth) was shown to be unrelated to changes in A_C. It should be noted that MARINO and MEHTA (1987) came to the same conclusion in their investigation of 18 inlets along the east coast of Florida. However, MARINO and MEHTA (1987) concluded that the ebb shoal volume is in part determined by an inlet's aspect ratio. Their study (MARINO and MEHTA, 1987), when focused on inlets of similar cross-sectional area, determined that an inverse relationship existed between V_{ETD} and aspect ratio. Larger ebb delta volume inlets were found to possess smaller aspect ratios than inlets with diminished ebb shoals. Thus, it was deduced that an overall decrease in the aspect ratio would be observed over time as a newly relocated inlet evolved. This study of the relocated Mason Inlet has not revealed such a clear-cut trend. Fluctuations in the aspect ratio were observed concurrent with the continual growth of the ebb delta (Tables 4 and 5). Reasons for observations such as these are varied but most likely relate to the severe adjustment initially and the potentially non-equilibrated inlet system. Perhaps when the ebb delta reaches a larger volume the aspect ratio may become a better-suited indicator of volume changes. KNIERIM's (2003) study of Rich Inlet suggested that changes in the aspect ratio for that system were a poor indicator of volume changes occurring on the ebb-tidal delta as well.

Analyzing the growth and development of the ebb-tidal delta can further determine whether or not the inlet achieved equilibrium within the period of study. The small difference (~1%) between the October 2002 V_{ETD} values estimated by ERICKSON *et al*. (2003) and that measured by the author serves to reinforce the confidence in the measured volumes of this study (Table 5). Equations 2 and 3, used in the prediction of V_{ETD}, were based on equilibrated inlet systems. Comparing the calculated V_{ETD} values (1.26×10^6 yd^3 and 1.04×10^6 yd^3) derived from Equations 2 and 3 with the actual delta size after 1.6 years from opening, it is seen that the inlet either had not reached equilibrium or did not necessarily conform to WALTON and ADAMS' (1976) model (Figure 21). The delta volume in October 2003 remained well below the predicted volume at approximately 309,859 yd^3 (between 24–30% of the predicted volume depending on the regression equation used). Inlet equilibration alone is not the only factor possibly accounting for this large discrepancy between the actual measured and predicted V_{ETD} values. Inlet size and behavior must also be considered since WALTON and ADAMS' (1976) regression analysis included a majority of inlets considerably larger and more locationally stable than Mason Inlet. KANA and MASON (1988) discussed this very issue at length in their study of Captain Sams Inlet's ebb-tidal delta formation. The Captain Sam's Inlet study attributed several factors besides equilibration for the observed difference in values. One of these factors was that many of the inlets used in WALTON and ADAMS' (1976) study were larger Florida and Texas microtidal inlets that were positioned along "mildly exposed" coasts and expected to exhibit less movement (KANA and MASON, 1988). Captain Sams Inlet is quite similar to Mason Inlet in that it is a relocated, small-migrating inlet whose ebb-tidal delta only attained 35% of the predicted volume

2.2 years after opening, with its channel appearing to have reached equilibrium relatively quickly. As a result, with regard to Mason Inlet, it is concluded that the ebb-tidal delta is most likely less than that predicted due to non-equilibrium and that the applicability of WALTON and ADAMS' (1976) equation is uncertain for an inlet of this size and migratory nature.

Based on the findings and time frame of this study, Mason Inlet may have failed to attain an equilibrated state with the surrounding forcing parameters. Several implications associated with the impacts of a non-equilibrated system should be considered, as the inlet will continue to adjust to its surroundings. As the ebb-tidal delta continues to increase in volume and the lagoon infills with sediment the neighboring shorelines will experience marked changes, mainly associated with erosion. The updrift shoreline of Figure Eight Island will likely continue to erode as sand will be transported to the ebb shoal and/or into the backbarrier channels. Based on historical behavior of the inlet, if left to its own devices it will migrate southwest at ever increasing rates as lagoonal infilling increases and tidal prism decreases. Migration would erode the northern extent of Wrightsville Beach, and Shell Island Resort could potentially be faced with a similar scenario already encountered in 1997.

To prevent history from repeating itself, some degree of inlet equilibrium must be attained. The system continues to be flood dominant and thus infills with sediment creating an unstable situation. As a result, the inlet migrates and erodes both shorelines in the process. Stipulations of the relocation agreement require the inlet to remain within a 1,000-ft corridor and allow dredging for this purpose. Dredging the inlet’s feeder channels will aid in keeping the inlet channel in place by providing a larger volume of tidal prism and flushing through the inlet throat. However, if that material is placed on the updrift shoreline of Figure Eight Island it will likely be transported back into the inlet or to the ebb shoal. Too much dredging could adversely compromise the Figure Eight Island enlarging T_P enough to cause the ebb-tidal delta to require more sand from the updrift shoreline. For this system, finding an equilibration state that works well for the entire system will be extremely challenging and expensive.

CONCLUSIONS

The study of Mason Inlet over 1.6 years following artificial relocation resulted in several conclusions that included:

- Opposing accretion/erosion trends observed before and after relocation are directly related to relocation of the inlet and the formation of the new ebb- and flood-tidal shoals.
- Cumulative erosion of both neighboring oceanfront shorelines, post-relocation, can be attributed to: 1) opening of a new inlet thereby causing reorientation of the shoreline; 2) morphologic alteration of the shoulders with inlet migration to the southwest; 3) collapse of the original ebb-tidal delta and exposure of the shoreline to unimpeded wave energy; 4) formation of a new ebb-tidal delta that retained sand from neighboring beaches, and; 5) development of interior flood shoals and infilling of the lagoon.
- Characteristic traits associated with flood dominance appear to be exhibited in this newly evolving inlet system. Key indicative traits include: 1) longer measured ebb durations than flood; 2) measured flood current velocities exceeding maximum thresholds for sediment transport; 3) ADCP-calculated flood flow volumes exceeding ebb flow volumes; 4) noticeable infilling of the backbarrier and measured movement of a flood shoal in a net landward direction with volumetric accumulation occurring simultaneously; 5) mean maximum flood velocity (0.73 ft/s) exceeding mean maximum ebb velocity (0.62 ft/s) within Banks Channel as measured by Erickson Consulting Engineers, Inc.,

and; 6) backbarrier morphology of a bay filled with high marsh. Most of these same traits were determined to exist prior to relocation and indicative of flood dominance.

- Mason Creek appears to be the dominant feeder channel capturing a larger percentage of flow distributed into the backbarrier during the flood portion of a tidal cycle. Dominance of this channel over Banks Channel is explained by the physical parameters that uniquely characterize each conduit and appears to be independent of tidal range and tidal prism. Characteristics such as cross-sectional area, shape, depth, channel alignment, and shoaling nature all favor a greater hydraulic efficiency through Mason Creek and appear to play a dominant role in dictating flow distribution.
- Tidal prism (T_P) is extremely variable in this evolving system and determined to be highly correlated to measured changes in cross-sectional area of the inlet throat ($r = 0.95$) and fluctuations in tidal range ($r = 0.87$).
- JARRETT's (1976) theoretical equation relating T_P and A_C appears to be a useful tool for estimation of the relocated Mason Inlet's T_P. ADCP-derived T_P estimates are most likely superior to the empirically derived estimations calculated from the theoretical equations of O'BRIEN (1931 and 1969) and JARRETT (1976). ADCP measurements are based on field data pertinent to the area of interest on a particular survey, whereas the regression equations exclude extraneous factors such as wind, waves, freshwater inputs, and other conditions that further complicate estimations. However, the estimates of both methods were found to be quite comparable with only 7% and 8% differences in values.
- Channel cross-sectional area (A_C) achieved a value of approximately 3,414 ft^2 within 477 days after opening. This value is within 7% of the area predicted by the theoretical

equation of JARRETT (1976). This A_C value (3,414 ft^2) may approximate the equilibrated channel section the inlet is attempting to attain.

- Aspect ratio (width:depth) of the inlet throat does not appear to be a good indicator of ebb-tidal delta volume changes for Mason Inlet.
- The volume of sand in the new ebb-tidal delta after 1.6 years remains well below (70–76% below) the equilibrium volume predicted by WALTON and ADAMS' (1976) empirical relationship. Explanations for this discrepancy are either related to the inlet's failure to attain equilibrium or its inability to conform to WALTON and ADAMS' (1976) empirical relationship due to its relatively small size and migratory nature.

LITERATURE CITED

Applied Technology and Management, 2000. Environmental Assessment of Mason Inlet Relocation Project, Wilmington, NC. Wilmington, North Carolina: Applied Technology and Management, 106p.

AUBREY, D. and SPEER, P., 1985. A study of non-linear tidal propagation in shallow inlet estuarine systems Part I: Observations. *In: Estuarine, Coastal and Shelf Science*, 21. pp. 185–205.

BOON III, J.D. and BYRNE, R.J., 1981. On basin hypsometry and the morphodynamic response of coastal inlet systems. *Marine Geology,* 40, 27–48.

BROOKS, W.B., 1988. A historic and morphologic study of Mason and Rich Inlets, North Carolina. Wilmington, North Carolina: University of North Carolina at Wilmington, Master's thesis, 87p.

BRUUN, P. and GERRITSEN, F., 1959. Natural bypassing of sand at coastal inlets. *Journal Waterways and Harbors Division*, New York: ASCE, 85, 75–107.

BUDDE, L.E. and CLEARY, W.J., 2004. Barrier progradation related to inlet spacing and migration patterns. *Journal of Coastal Research*, Special Issue No. 39, 5p.

BYRNE, R.J.; GAMMISCH, R.A., and THOMAS, G.R., 1980. Tidal prism area relations for small tidal inlets. *Proceedings of the Seventeenth Coastal Engineering Conference,* ASCE, Sydney, Australia, pp. 2517–2533.

BYRNES, M.R.; BAKER, J.L., and FENG, L., 2002. Quantifying potential measurement errors and uncertainties associated with bathymetric change analysis. *Coastal and Hydraulics Engineering Technical Note IV-50*, U.S. Army Corps of Engineers, Coastal Engineering Center & Waterways Experiment Station, Vicksburg, MS, 17p.

CLEARY, W.J.; HOSIER, P.E., and WELLS, G.R., 1979. Genesis and significance of marsh lands within southeastern North Carolina lagoons. *Journal of Sedimentary Petrology,*49(3), 703–710.

CLEARY, W.J.; HOSIER, P.E., and GAMMIL, S.P., 1989. Historic and dredging-induced shoreline changes, Bald Head Island, Cape Fear, NC. *Proceedings of Coastal Zone '89*, pp. 3017–3029.

CLEARY, W.J., 1996. Inlet induced shoreline changes: Cape Lookout - Cape Fear. *In* CLEARY, W.J. (ed.)*, Environmental Coastal Geology: Cape Lookout to Cape Fear, N.C.* Carolina Geological Society, pp. 49–60.

CLEARY, W.J. and MARDEN, T.P., 1999. Shifting Shorelines: A Pictorial Atlas of North Carolina Inlets. Raleigh, North Carolina: N.C. Sea Grant Publication No.99-X, 60p.

CLEARY, W.J. and FITZGERALD, D.M., 2003. Tidal inlet response to natural sedimentation processes and dredging-induced tidal prism changes: Mason Inlet, North Carolina. *Journal of Coastal Research*, 19(4), 1018–1025.

CONCEJO, A.V., 2003. Sediment Dynamics and Tidal Inlet Relocation in Mixed-Energy Settings: The case of Ancão Inlet (Algarve, Portugal). Algarve, Portugal: University of Algarve, Ph.D. thesis, 197p.

CROWELL, M.; LEATHERMAN, S.P., and BUCKLEY, M.K., 1991. Historical shoreline change: error analysis and mapping accuracy. *Journal of Coastal Research,* 7(3), 839–852.

DAVIS, R.A.; HINE, A.C., and BLAND, M.J., 1987. Midnight Pass, Florida: inlet instability due to man-related activities in Little Sarasota Bay. *Proceedings of Coastal Sediments '87,* American Society of Civil Engineers, New York, N.Y., pp. 2062–2077.

DEAN, R.G. and WALTON, T.L., JR., 1975. Sediment transport processes in the vicinity of inlets with special references to sand trapping. *In:* Cronin, L.E. (ed.), *Estuarine Research*, vol. 2, New York: Academic Press, pp. 129–150.

DOLAN, R., HAYDEN, B.P. and HEYWOOD, J., 1978. A new photogrammetric method for determining shoreline erosion. *Coastal Engineering*, 2, 21–39.

DOLAN, R., HAYDEN, B.P., MAY, P. and MAY, S., 1980. The reliability of shoreline change measurements from aerial photographs. *Shore and Beach*, 48(4), 22–29.

ERICKSON, K.M.; KRAUS, N.C., and CARR, E.E., 2003. Circulation change and ebb shoal development following relocation of Mason Inlet, North Carolina. *Proceedings of Coastal Sediments '03,* (Clearwater Beach, Florida), CD-ROM.

Erickson Consulting Engineers Staff, 2003. Midnight Pass Reopening Project. Erickson Consulting Engineers, Inc., Technical Report, 43p.

FINLEY, R.S., 1976. Hydraulics and dynamics of North Inlet, South Carolina, 1974-1975. Fort Belvoir, Virginia: U.S. Army Corps of Engineers, *GITI Report #10,* 214p.

FITZGERALD, D.M.; NUMMEDAL, D., and KANA, T., 1976. Sand circulation patterns at Price Inlet, South Carolina. *Proceedings 15th Coastal Engineering Conference,* American Society of Civil Engineers, pp. 1868–1880.

FITZGERALD, D.M.; HUBBARD, D.K., and NUMMEDAL, D., 1978. Shoreline changes associated with tidal inlets along the South Carolina coast. *In: Coastal Zone '78*, San Francisco, CA, American Society of Civil Engineers, pp. 1973–1994.

FITZGERALD, D.M., 1982. Sediment bypassing at mixed energy tidal inlets. *Proceedings of the 18th International Conference of Coastal Engineering* (Cape Town, South Africa, ASCE), pp. 1094–1118.

FITZGERALD, D.M., 1988. Shoreline erosional-depositional processes associated with tidal inlets. *In*: Aubrey, D.G. and Weishar, L. (eds.), *Hydrodynamics and Sediment Dynamics of Tidal Inlets, Lecture Notes on Coastal and Estuarine Studies*, 29. New York: Springer-Verlag, pp. 186–225.

FITZGERALD, D.M., 1996. Geomorphic variability and morphologic and sedimentologic controls on tidal inlets. *Journal of Coastal Research,* Special Issue No. 23, 47–71.

FREEMAN, C.W., 2001. Backbarrier Sedimentation and Inlet Induced Shoreline Change Associated with a Migrating Tidal Inlet: Mason Inlet, North Carolina. Wilmington, North Carolina: University of North Carolina at Wilmington, Master's thesis, 77p.

FRIEDRICHS, C.; LYNCH, D., and AUBREY, D., 1992. Velocity asymmetries in frictionally-dominated tidal embayments: longitudinal and lateral variability. *In:* Prandle, D. (ed.), *Coastal and Estuarine Studies.* Washington, D.C., pp. 277–312.

Gahagan and Bryant Associates Staff, 2002. Mason Inlet Monitoring Project, Hydrographic Monitoring Data, Asbuilt – July 2002. Wilmington, North Carolina: Gahagan and Bryant Associates, Inc., Technical Report, 109p.

HAYES, M.O., 1975. Morphology of sand accumulation in estuaries: an introduction to the symposium. *In: Geology and Engineering, Estuarine Research Collection, 2.* New York: Academic Press, pp. 3–22.

HAYES, M.O., 1979. Barrier island morphology as a function of tidal and wave regime. *In:* Leatherman, S.P. (ed.), *Barrier Island: From the Gulf of St. Lawrence to the Gulf of Mexico.* New York: Academic, pp. 1–28.

HAYES, M.O., 1980. General morphology and sediment patterns in tidal inlets. *Sedimentary Geology*, 26, 139–156.

HAYES, M.O., 1994. The Georgia Bight barrier system. *In*: Davis, Jr. R.A. (ed.), *Geology of Holocene BarrierIsland Systems*, 7. New York: Springer-Verlag, pp. 233–304.

HICKS, D.M. and HUME, T.M., 1997. Determining sand volumes and bathymetric change of an ebb-tidal shoal. *Journal of Coastal Research*, 13(2), 407–416.

JACKSON, C.W., 2004. Quantitative Shoreline Change Analysis of an Inlet-Influenced Transgressive Barrier System: Figure Eight Island, North Carolina. Wilmington, North Carolina: University of North Carolina at Wilmington, Master's thesis, 95p.

JARRETT, J.T., 1976. Tidal prism-inlet area relationships. Fort Belvoir, Virginia and Vicksburg, Mississippi: U.S. Army Corps of Engineers, Coastal Engineering Center and Waterways Experiment Station, *GITI Report #3*, 76p.

JARRETT, J.T., 1977. Sediment budget analysis, Wrightsville Beach to Kure Beach, N.C. *Proceedings of Coastal Sediments, '77,* American Society of Civil Engineers, New York, NY, pp. 986–1005.

JOHNSEN, C.D.; CLEARY, W.J.; FREEMAN, W.C., and SAULT, M., 1999. Inlet induced shoreline changes on the high-energy flank of the Cape Fear Foreland, N.C. *Proceedings of Coastal Sediments '99,* American Society of Civil Engineers, New York, N.Y., pp. 1402–1418.

JOHNSON, J., 1919. Shore Processes and Shoreline Development: New York, NY: John Wiley & Sons, 584p.

KANA, T.W.; MASON, J.E., and WILLIAMS, M.L., 1987. A sediment budget for a relocated tidal inlet. *Proceedings of Coastal Sediments '87,* American Society of Civil Engineers, New York, N.Y., pp. 2094–2109.

KANA, T.W. and MASON, J.E., 1988. Evolution of an ebb-tidal delta after an inlet relocation. *In*: Aubrey, D.G. and Weishar, L. (eds.), *Hydrodynamics and Sediment Dynamics of Tidal Inlets, Lecture Notes on Coastal and Estuarine Studies*, 29. New York: Springer-Verlag, pp. 382–411.

KANA, T.W.; HAYTER, E.J., and WORK, P.A., 1999. Mesoscale sediment transport at southeastern U.S. tidal inlets: conceptual model applicable to mixed energy settings. *Journal of Coastal Research,* 15(2), 303–313.

KANA, T.W. and MCKEE, P.A., 2003. Relocation of Captain Sams Inlet – 20 years later. *Proceedings of Coastal Sediments '03,* (Clearwater Beach, Florida), CD-ROM.

KNIERIM, A.C., 2003. Hydrographic Investigation of a Wave-Influenced Mixed Energy Inlet: Rich Inlet, North Carolina. Wilmington, North Carolina: University of North Carolina at Wilmington, Master's thesis, 51p.

KRAUS, N.C., ZARILLO, G.A. and TAVOLARO, J.F., 2003. Hypothetical relocation of Fire Island Inlet, New York. *Proceedings of Coastal Sediments '03,* (Clearwater Beach, Florida), CR-ROM.

LECONTE, L.J., 1905. Discussion of "Notes on the Improvement of River and Harbor Outlets in the United States," Paper No. 1009 by D.A. Watts, Transactions, American Society of Civil Engineers, Vol. LV, Dec. 1905, pp. 306–308.

LINCOLN, J. and FITZGERALD, D., 1988. Tidal distortions and flood dominance at five small tidal inlets in southeastern Maine. *Marine Geology*, 82, 133–148.

MANNING, R., 1891. *On the Flow of Water in Open Channels and Pipes.* Transactions of the Institution of Civil Engineers of Ireland.

MARINO, J.N., 1986. Inlet ebb shoal volumes related to coastal physical parameters. Gainesville, Florida: University of Florida, Gainesville, Coastal and Oceanographic Engineering Department, *UFL/COEL-86-017*, 116p.

MARINO, J.N. and MEHTA, J.A., 1987. Inlet ebb shoals related to coastal parameters. *Proceedings of Coastal Sediments '87,* American Society of Civil Engineers, New York, N.Y., pp. 1608–1623.

MEYER-PETER, E. and MULLER, R., 1948. Formulas for bed-load transport. 2nd Meeting IAHR, pp. 39–64.

MILLER, M.C.; MCCAVE, I.N., and KOMAR, P.D., 1977. Threshold of sediment motion under unidirectional currents. *Sedimentology,* 24, 507–527.

MILITELLO, A., and KRAUS, N.C., 2001. *Shinnecock Inlet, New York, Site Investigation, Report 4, Evaluation of Flood and Ebb Shoal Sediment Source Alternatives for the West of Shinnecock Interim Project, New York.* Coastal Inlets Research Program, Technical Report ERDC-CHL-TR-98-32. U.S. Army Engineer Research and Development Center, Vicksburg, Mississippi.

MORLOCK, S.E., 1996. Evaluation of Acoustic Doppler Current Profiler Measurements of River Discharge. Indianapolis, Indiana: U.S. Geological Survey, *Water-Resources Investigations Report 95-4218*, 41p.

MOTA OLIVEIRA, I., 1970. Natural flushing ability of tidal inlets. *12th Conference on Coastal Engineering*, pp. 1827–1845.

National Data Buoy Center, 2003. Historical Standard Meteorological Data (2003). Available from World Wide Web <http://www.ndbc.noaa.gov/station_history.phtml?station=fpsn7>. ASCII format.

National Flood Insurance Program, 2003. *Vertical Datum Changes: North Carolina.* FEMA's cooperating technical partner. Available from World Wide Web <http://www.ncfloodmaps.com/pubdocs/datum_conversion.pdf>. PDF format.

NAYAK, I.V., 1971. Tidal Prism - Area Relationship in a Model Inlet. Berkely, California: University of California at Berkely, Hydraulic Engineering Laboratory, *Technical Report HEL 24-1*.

O'BRIEN, M.P., 1931. Estuary tidal prisms related to entrance areas. *Civil Engineering*, 1(8), 738–739.

O'BRIEN, M.P., 1969. Equilibrium flow areas of inlets on sandy coasts. *Journal Waterways and Harbors Division*, New York: ASCE, 95, 43–52.

OERTEL, G.F., 1975. Ebb-tidal deltas of Georgia estuaries. *In:* Cronin, L.E. (ed.), *Estuarine Research*, vol. 2, New York: Academic Press, pp. 267–276.

OERTEL, G.F., 1977. Geomorphic cycles in ebb deltas and related patterns of shore erosion and accretion. *Journal of Sedimentary Petrology,* 47(3), 1121–1131.

PAJAK, M.J. and LEATHERMAN, S., 2002. The high water line as shoreline indicator. *Journal of Coastal Research*, 18(2), 329–337.

POFF, M.T., 2004. Personal Communication. Coastal Engineering Consultants, Inc., Naples, Florida.

RD Instruments, 2003. WinRiver User's Guide, International Version. San Diego, California: RD Instruments, *Technical Report P/N 957-6171-00*, 159p.

STAUBLE, R.K., 1998. Techniques for measuring and analyzing inlet ebb-shoal evolution. *Coastal Engineering Technical Note IV-13*, U.S. Army Corps of Engineers, Coastal Engineering Center & Waterways Experiment Station, Vicksburg, MS, 12p.

U.S. Army Corps of Engineers, 1982. Feasibility Report and Environmental Assessment of Shore and Hurricane Wave Protection, Wrightsville Beach, North Carolina. Wilmington, North Carolina: U.S. Army Corps of Engineers Publication.

U.S. Army Corps of Engineers, 2003. Engineering analysis at tidal inlets. *Proceedings of 4th Annual Tech-transfer Workshop '03,* Coastal Inlets Research Program, 26p. Available from World Wide Web <http://cirp.wes.army.mil/cirp/presentations/fsb03/Seabergh_EngAnalysis2003_H2.pdf>. PDF format.

VILA, A.; ALVEIRINHO DIAS J.M.; FERREIRA, O., and MATIAS, A., 1999. Natural evolution of an artificial inlet. *Proceedings of Coastal Sediments '99*, American Society of Civil Engineers, New York, N.Y., pp. 1478–1488.

WALTON, T.L., Jr. and ADAMS, W.D., 1976. Capacity of inlet outer bars to store sand. *Proceedings of the 15th Conference of Coastal Engineering* (New York, New York, ASCE), 2, pp. 1919–1937.

Waterway Surveys & Engineering, Ltd.; Olsen Associates, Inc., and Lent, L.K., 2001. Rudee Inlet Management Study, CIP 8-301. Virginia Beach, Virginia: Technical Report, 108p.

ZARILLO, G., 1986. Tidal dynamics and substrate response in a salt-marsh estuary. *Marine Geology,* 67, 13–35.

ZARILLO, G.A. and MILITELLO, A., 1999. Ponce de Leon Inlet, Florida, Site Investigation. Report 2: Inlet Hydrodynamics: Monitoring and Interpretation of Physical Processes. Technical Report CHL-99-1. U. S. Army Engineer Waterways Experiment Station, Vicksburg, Mississippi.